# Ion traps in nuclear physics

Mathias Gerbaux
gerbaux@cenbg.in2p3.fr

Centre d'Études Nucléaires de Bordeaux-Gradignan

École Joliot-Curie 2021

# Merci aux organisateurs !

PIPERADE

PIEGES DE PENNING POUR LES RADIONUCLEIDES A DESIR

P. Ascher, L. Daudin, A. de Roubin, M. Flayol,
S. Grévy, M. Hukkanen, A. Husson, B. Lachacinski

# Questions welcome all along the lecture !

# Outline

# A (very) brief history

Frans Michel Penning

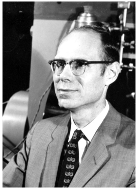

John Robinson Pierce

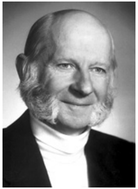

Hans Georg Dehmelt

Wolfgang Paul

- 1936 : first Penning vacuum gauge
- 1949 : J.R. Pierce discuss the principle of a "magnetron trap" in his book about $e^-$ beams
- 1953 : W. Paul builds the first quadrupole RF mass spectrometer
- 1959 : First Penning trap by H.G. Dehmelt
- 1986 : complete geonium theory by L. Brown and G. Gabrielse
- 1987 : first radionuclide mass measurement in a Penning trap (ISOLTRAP)

# What are traps used for ?

- Traps are used in a wide variety of domains
- Main application : mass spectrometry
- Several topics (at least partly) in the scope of IN2P3
  - Nuclear physics
  - Beam preparation
  - Standard Model tests
  - Antimatter studies

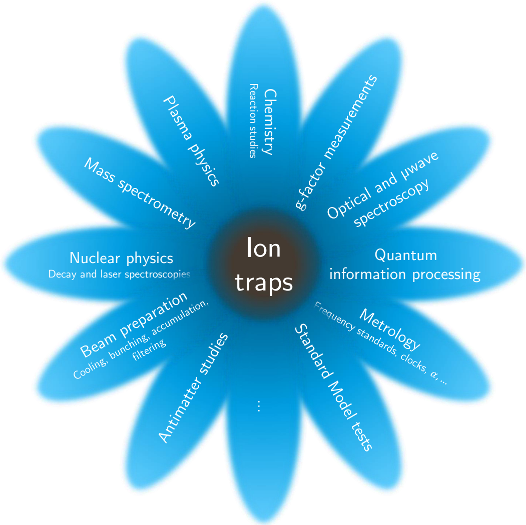

# Beams in nuclear physics - ISOL vs in-flight methods

High energy (~GeV/u) and fast (μs)

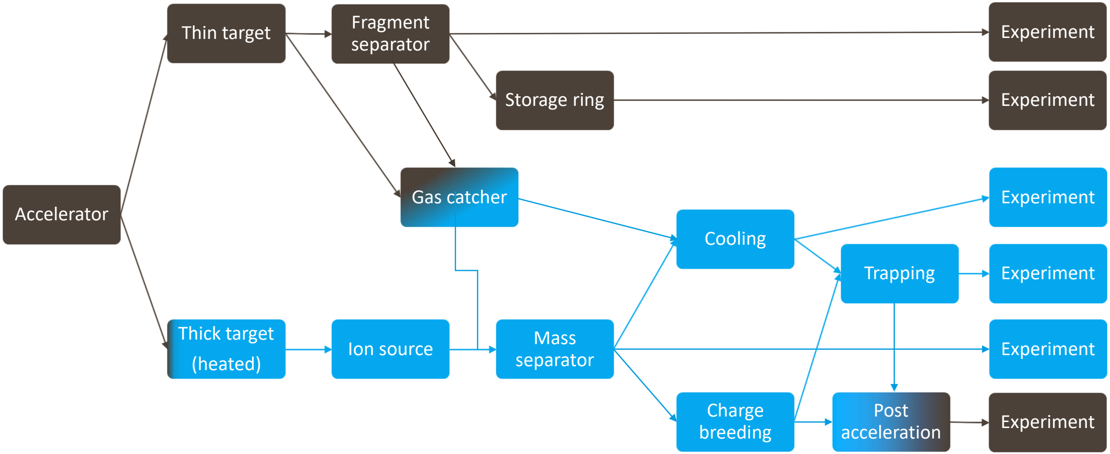


Low energy (meV - 100 keV/u) and rather slow (ms to s)

# Beams in nuclear physics - ISOL vs in-flight methods

## ISOL

- Beams usually have a single charge state and a low energy dispersion

## In-flight

- Beams have a whole distribution of charge states and momentum

# Beams in nuclear physics - ISOL vs in-flight methods

## ISOL

- Beams usually have a single charge state and a low energy dispersion
- Method is intrinsically slow (effusion-diffusion from target to source)

## In-flight

- Beams have a whole distribution of charge states and momentum
- Method is intrinsically fast (beam is never stopped)

# Beams in nuclear physics - ISOL vs in-flight methods

## ISOL

- Beams usually have a single charge state and a low energy dispersion
- Method is intrinsically slow (effusion-diffusion from target to source)
- production of refractory elements by ISOL method is very challenging

## In-flight

- Beams have a whole distribution of charge states and momentum
- Method is intrinsically fast (beam is never stopped)
- Insensitive to the chemistry of the element of interest

# Emittance

- ”Quality” of the beam is a key parameter for trapping
- This is described by the emittance concept

# Emittance

- ”Quality” of the beam is a key parameter for trapping
- This is described by the emittance concept
- Emittance is the spread of the beam in the phase space
- In the absence of dissipative forces emittance is conserved

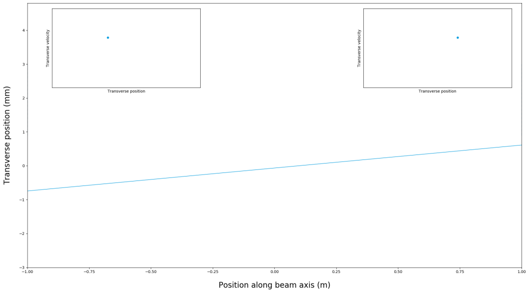

# Emittance

- ”Quality” of the beam is a key parameter for trapping
- This is described by the emittance concept
- Emittance is the spread of the beam in the phase space
- In the absence of dissipative forces emittance is conserved

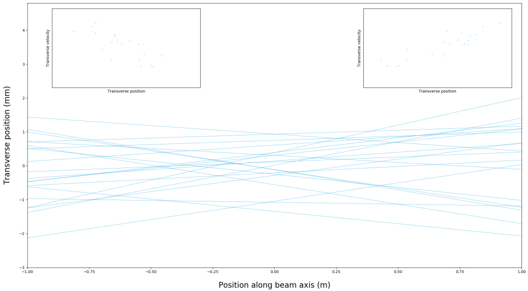

# Emittance

- "Quality" of the beam is a key parameter for trapping
- This is described by the emittance concept
- Emittance is the spread of the beam in the phase space
- In the absence of dissipative forces emittance is conserved

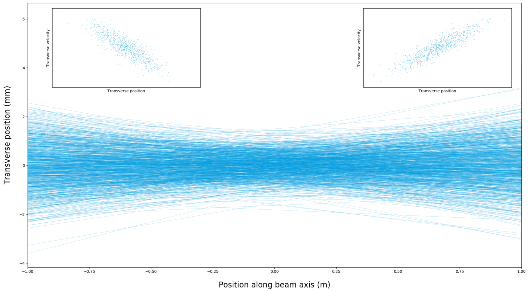

# Emittance

- ”Quality” of the beam is a key parameter for trapping
- This is described by the emittance concept
- Emittance is the spread of the beam in the phase space
- In the absence of dissipative forces emittance is conserved
- A typical beam has its particle grouped within an ellipse in the phase space with a tilt depending on the focusing

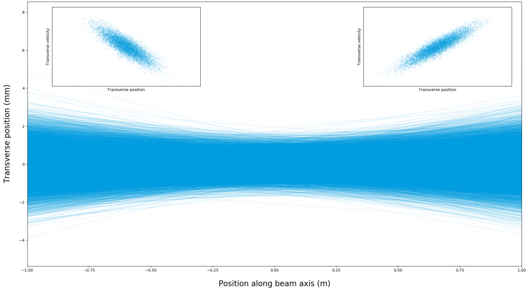

# Why it is needed to prepare the beam

- Radioactive ion beams production facilities usually deliver...
  - beams with typical emittance $\varepsilon \simeq$ a few $10\pi.mm.mrad$
  - (quasi-)continuous beams
- Efficient injection into a trap requires...
  - $\varepsilon \lesssim$ a few $\pi.mm.mrad$
  - A bunched beam with a duration between ion bunches ranging from ms to s

The beam must be cooled and bunched before trapping !

# Why it is needed to purify the beam

- Suppose one want to measure the half-life of a given nucleus ($^{62}$Ga)

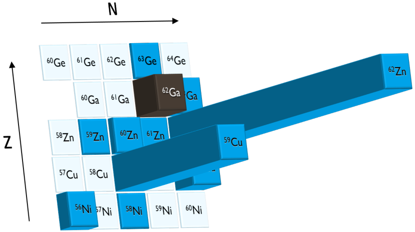

# Why it is needed to purify the beam

- Suppose one want to measure the half-life of a given nucleus ($^{62}$Ga)
- A contaminated sample will result in a biased measurement

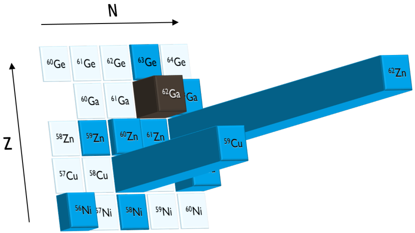


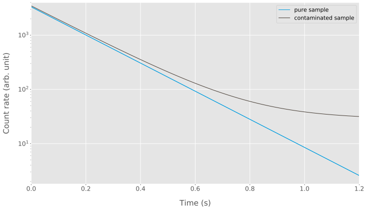

# Why it is needed to purify the beam

- Suppose one want to measure the half-life of a given nucleus ($^{62}$Ga)
- A contaminated sample will result in a biased measurement
- Mass is a specific feature of each nucleus (and even nuclear state)

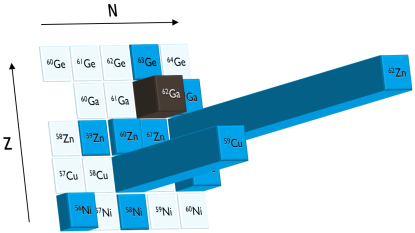


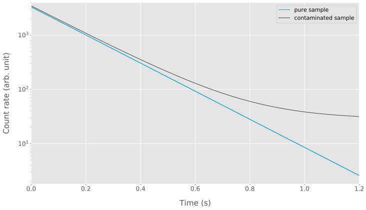

# Why it is needed to purify the beam

- Suppose one want to measure the half-life of a given nucleus ($^{62}$Ga)
- A contaminated sample will result in a biased measurement
- Mass is a specific feature of each nucleus (and even nuclear state)
- Selecting using $Q/m$ is the usual technique since J. J. Thomson's discovery of the Neon isotopes

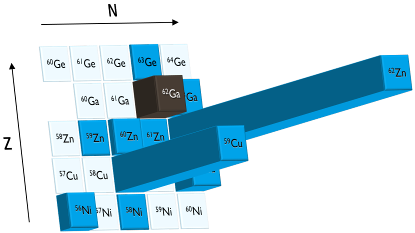


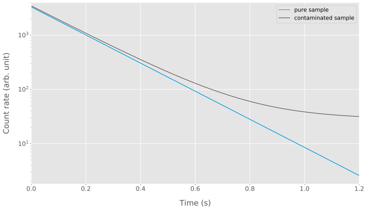

# Mass resolution

Mass resolution $R = \dfrac{M}{\Delta M}$ describes the ability to separate nuclides with close masses

- Makes really sense only for ISOL-like beams
- A simple dipole magnet has $R \approx$ a few 100
- A high resolution separator can reach $R \sim 10^4$

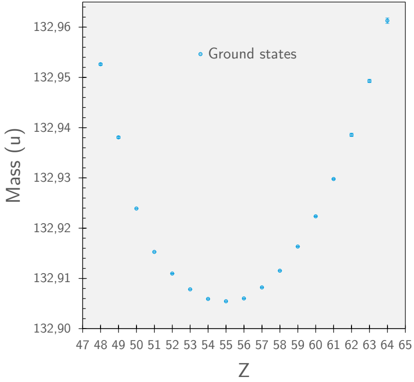


Even a HRS is sometimes not enough to separate isobars (not speaking about nuclear isomers)

# Mass resolution

Mass resolution $R = \dfrac{M}{\Delta M}$ describes the ability to separate nuclides with close masses

- Makes really sense only for ISOL-like beams
- A simple dipole magnet has $R \approx$ a few 100
- A high resolution separator can reach $R \sim 10^4$

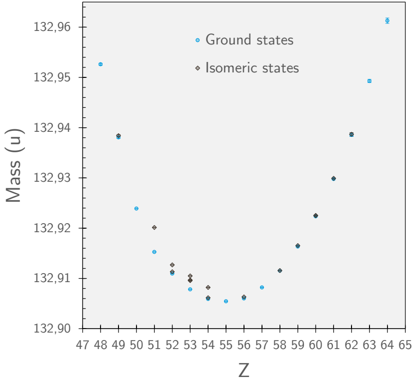


Even a HRS is sometimes not enough to separate isobars (not speaking about nuclear isomers)

# What "traps" will we talk about ?

- Many types of charged particle traps exist but few of them used in our field
- We will focus on the low-energy ($<$ a few 10 keV) nuclear physics tools i.e.
  - Paul traps
  - Penning traps
  - MR-ToF MS
- We will hence not discuss storage rings

# Trap setups dedicated to nuclear physics

# Trapping charged particles almost at rest

# Trapping with an electrostatic field ?

- Starting from Maxwell-Gauss law
  $\overrightarrow{\nabla} \cdot \vec{E} = \frac{\rho}{\varepsilon}$
- In vacuum and for an electrostatic field, it simplifies to $\overrightarrow{\nabla} \cdot \vec{E} = \nabla^2 V = 0$
- There is hence no local maximum or minimum of the electric potential $V$, one can at best obtain a saddle point

# Trapping with an electrostatic field ?

- Starting from Maxwell-Gauss law $\vec{\nabla} \cdot \vec{E} = \frac{\rho}{\varepsilon}$
- In vacuum and for an electrostatic field, it simplifies to $\vec{\nabla} \cdot \vec{E} = \nabla^2 V = 0$
- There is hence no local maximum or minimum of the electric potential $V$, one can at best obtain a saddle point
- Saddle electric potential confines charged particles in one direction...
- but the particles can escape in the other direction

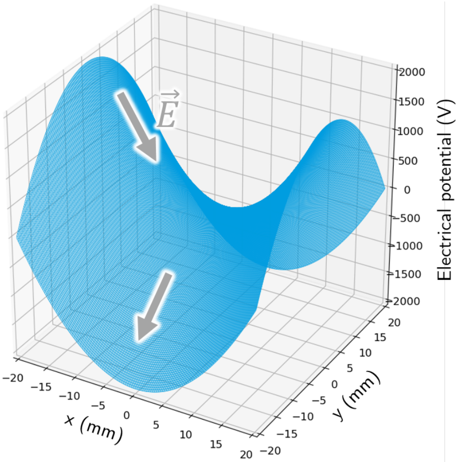


**Earnshaw's theorem (1842)**

It is not possible to trap charged particles in all three dimensions with an electrostatic field

The same can be demonstrated for a magnetostatic field

# Cheating with Earnshaw's theorem

- We will see later that ions can be trapped in a purely electrostatic device (MR-ToF MS)
- This is *not* in contradiction with Earnshaw's theorem
- In a MR-ToF MS, the kinetic energy of the ions can not be reduced to ≈0 ⇒in the ion reference frame, the $\vec{E}$ field is *not* static

# Two approaches for (real) trapping

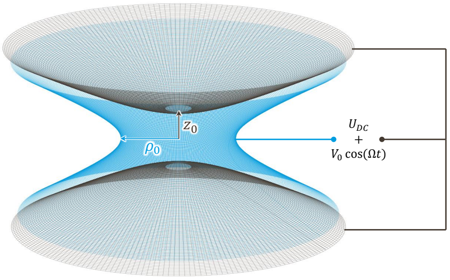


Paul trap

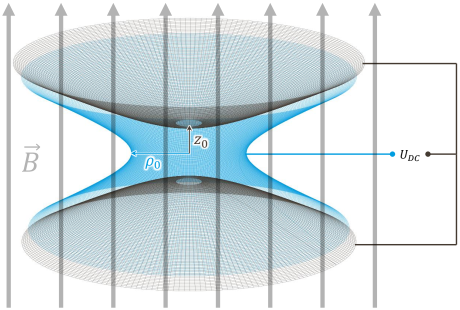


Penning trap

# Trap geometries

The theoretical ideal shape for both Penning and 3D Paul trap is made of hyperboloids of revolution (1 sheet + 2 sheets) but...

# Trap geometries

The theoretical ideal shape for both Penning and 3D Paul trap is made of hyperboloids of revolution (1 sheet + 2 sheets) but...

- Hard to machine

# Trap geometries

The theoretical ideal shape for both Penning and 3D Paul trap is made of hyperboloids of revolution (1 sheet + 2 sheets) but...

- Hard to machine
- No easy access inside

# Trap geometries

The theoretical ideal shape for both Penning and 3D Paul trap is made of hyperboloids of revolution (1 sheet + 2 sheets) but...

- Hard to machine
- No easy access inside
- Requires at least one hole (usually two) for beam injection
- Electrodes extending to infinity are not very handy !

# Trap geometries

The theoretical ideal shape for both Penning and 3D Paul trap is made of hyperboloids of revolution (1 sheet + 2 sheets) but...

- Hard to machine
- No easy access inside
- Requires at least one hole (usually two) for beam injection
- Electrodes extending to infinity are not very handy !

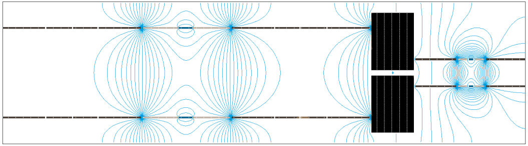

Many traps made of cylindrical electrodes with potentials finely tuned to approach the ideal case near the center of the trap

# Paul traps

# Potential inside a Paul trap

- Saddle electric potential (hyperbolic paraboloid) confines charged particles in one direction...
- but the particles can escape in the other direction
- This can be avoided if the potential is flapped fast enough !

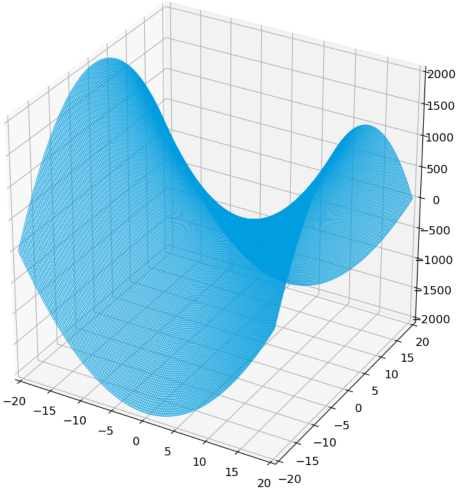

# Motion of charged particles in a Paul trap

The most desirable restoring force is one proportional to the distance from the center of the trap.
The electric potential will hence have the form :

$$\Phi \propto \lambda x^2 + \mu y^2 + \nu z^2$$

To obey Laplace's equation $\Delta\Phi = 0$, 2 solutions are used :

$$\begin{cases} \lambda = \mu = +1 \text{ and } \nu = -2 & \text{corresponding to a 3D Paul trap} \\ \lambda = -\mu = +1 \text{ and } \nu = 0 & \text{corresponding to a linear Paul trap} \end{cases}$$

# Motion of charged particles in a 3D Paul trap

As a time-varying potential is needed, the one of a 3D Paul trap generally has the form :

$$\Phi = [U_{DC} + V_0 \cos(\Omega t)] \frac{x^2 + y^2 - 2z^2}{4d_0^2}$$

where...

- $d_0^2 = \frac{z_0^2}{2} + \frac{\rho_0^2}{4}$
- $\Omega$ is the driving RF angular frequency

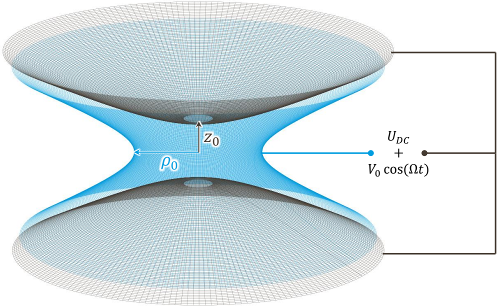


Note that the DC part is not mandatory for trapping

# Motion of charged particles in a 3D Paul trap

The equation of motion of a particle with charge Q inside a Paul trap are :

$$\begin{cases} \ddot{x} + \dfrac{Q}{md_0^2}\left[U_{DC} + V_0 \cos\left(\Omega t\right)\right] x = 0 \\ \ddot{y} + \dfrac{Q}{md_0^2}\left[U_{DC} + V_0 \cos\left(\Omega t\right)\right] y = 0 \\ \ddot{y} + \dfrac{2Q}{md_0^2}\left[U_{DC} + V_0 \cos\left(\Omega t\right)\right] z = 0 \end{cases}$$

# Motion of charged particles in a 3D Paul trap

The equation of motion of a particle with charge Q inside a Paul trap are :

$$\begin{cases} \ddot{x} + \dfrac{Q}{md_0^2}\left[U_{DC} + V_0 \cos\left(\Omega t\right)\right] x = 0 \\ \\ \ddot{y} + \dfrac{Q}{md_0^2}\left[U_{DC} + V_0 \cos\left(\Omega t\right)\right] y = 0 \\ \\ \ddot{y} + \dfrac{2Q}{md_0^2}\left[U_{DC} + V_0 \cos\left(\Omega t\right)\right] z = 0 \end{cases}$$

That can be put in the compact form :

**Mathieu's equation**

$$\ddot{u} + \left[a_u - 2q_u \cos\left(2\tau\right)\right] u = 0$$

where $u = x$ , $y$ or $z$, and :

$$\begin{cases} a_x = a_y = \dfrac{-a_z}{2} = \dfrac{4U_{DC}}{d_0^2\Omega^2}\dfrac{Q}{m} \\ \\ q_x = q_y = \dfrac{-q_z}{2} = \dfrac{2V_0}{d_0^2\Omega^2}\dfrac{Q}{m} \\ \\ \tau = \dfrac{\Omega t}{2} \end{cases}$$

# Motion of charged particles in a 3D Paul trap

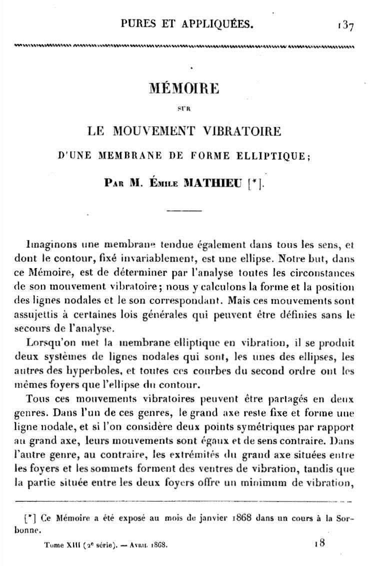
PURES ET APPLIQUÉES. 137

MÉMOIRE

SUR

LE MOUVEMENT VIBRATOIRE

D'UNE MEMBRANE DE FORME ELLIPTIQUE;

PAR M. ÉMILE MATHIEU [*].

Imaginons une membrane tendue également dans tous les sens, et dont le contour, fixé invariablement, est une ellipse. Notre but, dans ce Mémoire, est de déterminer par l'analyse toutes les circonstances de son mouvement vibratoire; nous y calculons la forme et la position des lignes nodales et le son correspondant. Mais ces mouvements sont assujettis à certaines lois générales qui peuvent être définies sans le secours de l'analyse.

Lorsqu'on met la membrane elliptique en vibration, il se produit deux systèmes de lignes nodales qui sont, les unes des ellipses, les autres des hyperboles, et toutes ces courbes du second ordre ont les mêmes foyers que l'ellipse du contour.

Tous ces mouvements vibratoires peuvent être partagés en deux genres. Dans l'un de ces genres, le grand axe reste fixe et forme une ligne nodale, et si l'on considère deux points symétriques par rapport au grand axe, leurs mouvements sont égaux et de sens contraire. Dans l'autre genre, au contraire, les extrémités du grand axe situées entre les foyers et les sommets forment des ventres de vibration, tandis que la partie située entre les deux foyers offre un minimum de vibration,

[*] Ce Mémoire a été exposé au mois de janvier 1868 dans un cours à la Sorbonne.

Tome XIII (2e série). — AVRIL 1868. 18

That can be put in the compact form :

**Mathieu's equation**

$$\ddot{u} + \left[a_u - 2q_u \cos(2\tau)\right] u = 0$$

where $u = x$ , $y$ or $z$, and :

$$\begin{cases} a_x = a_y = \dfrac{-a_z}{2} = \dfrac{4U_{DC}}{d_0^2\Omega^2}\dfrac{Q}{m} \\ q_x = q_y = \dfrac{-q_z}{2} = \dfrac{2V_0}{d_0^2\Omega^2}\dfrac{Q}{m} \\ \tau = \dfrac{\Omega t}{2} \end{cases}$$

# Stability inside a 3D Paul trap

Solutions have the form :

$$f_{\pm}(\tau) = \exp\left(\pm\left[\alpha_u + i\beta_u\right]\tau\right) g(\pm\tau)$$

Which are stables (i.e. non diverging if $\tau \to \infty$) only if $\alpha_u = 0$ and $\beta_u \neq n \in \mathbb{N}$

# Stability inside a 3D Paul trap

Solutions have the form :

$$f_{\pm}(\tau) = \exp\left(\pm\left[\alpha_u + i\beta_u\right]\tau\right) g(\pm\tau)$$

Which are stables (i.e. non diverging if $\tau \to \infty$) only if $\alpha_u = 0$ and $\beta_u \neq n \in \mathbb{N}$

- $\beta_u$ has a complicated expression that depends only on $a$ and $q$ $\Longrightarrow$ stability diagram
- The boundaries of the stable regions are those for which $\beta_u = n \in \mathbb{N}$

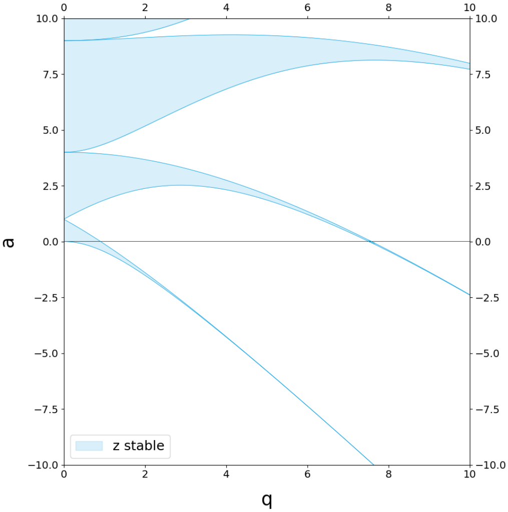


Stability of the solution hence depends on $Q/m$, $d_0$, $\Omega$, $U_{DC}$ and $V_0$

# Stability inside a 3D Paul trap

Solutions have the form :

$$f_{\pm}(\tau) = \exp\left(\pm\left[\alpha_u + i\beta_u\right]\tau\right) g(\pm\tau)$$

Which are stables (i.e. non diverging if $\tau \rightarrow \infty$) only if $\alpha_u = 0$ and $\beta_u \neq n \in \mathbb{N}$

- $\beta_u$ has a complicated expression that depends only on $a$ and $q$ $\Longrightarrow$ stability diagram
- The boundaries of the stable regions are those for which $\beta_u = n \in \mathbb{N}$

Stability of the solution hence depends on $Q/m$, $d_0$, $\Omega$, $U_{DC}$ and $V_0$

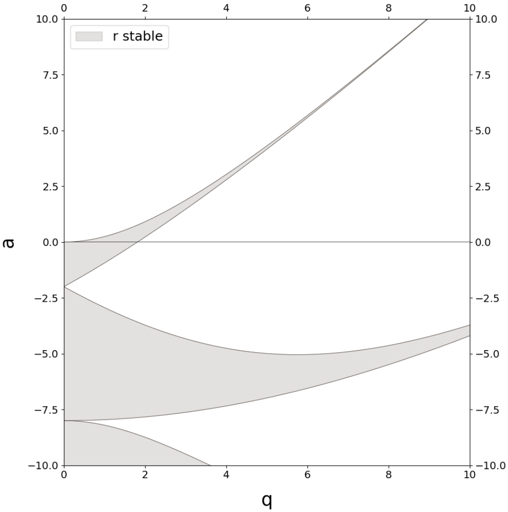

# Stability inside a 3D Paul trap

Solutions have the form :

$$f_{\pm}(\tau) = \exp\left(\pm\left[\alpha_u + i\beta_u\right]\tau\right) g(\pm\tau)$$

Which are stables (i.e. non diverging if $\tau \to \infty$) only if $\alpha_u = 0$ and $\beta_u \neq n \in \mathbb{N}$

- $\beta_u$ has a complicated expression that depends only on $a$ and $q$ $\implies$ stability diagram
- The boundaries of the stable regions are those for which $\beta_u = n \in \mathbb{N}$

Stability of the solution hence depends on $Q/m$, $d_0$, $\Omega$, $U_{DC}$ and $V_0$

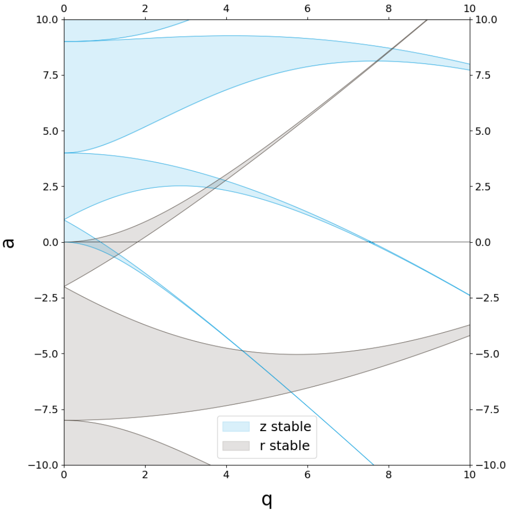

# Stability inside a 3D Paul trap

Stability of the solution hence depends on $Q/m$, $d_0$, $\Omega$, $U_{DC}$ and $V_0$

Usually, the "first" stability region is used

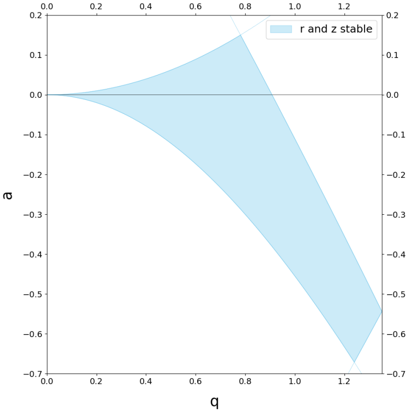


For $a = 0$, the motion is stable for $0 < q \lesssim 0.908$

For a $m = 100$ u ion and a $d_0 = 1\,\text{cm}$ trap if $U_{DC} = 0$, that means :

- If $V_0 = 100\,\text{V}$, motion is stable for $f = \frac{\Omega}{2\pi} > 328\,\text{kHz}$
- If $f = \frac{\Omega}{2\pi} = 1\,\text{MHz}$, motion is stable for $V_0 < 929\,\text{V}$

# Motion inside a 3D Paul trap

If the stablity condition is met, the solutions have the form :

$$u(\tau) = A \sum_{n=-\infty}^{\infty} c_{2n} \cos\left[(\beta_u + 2n)\,\tau\right] + B \sum_{n=-\infty}^{\infty} c_{2n} \sin\left[(\beta_u + 2n)\,\tau\right]$$

Where $c_{2n}$ depends on $a_u$ and $q_u$

The spectrum of the ion's motion hence contains the frequencies :

$$\omega_{u,n} = (\beta_u + 2n)\,\frac{\omega}{2} = \frac{\beta_u \Omega}{2} + n\Omega = \omega_{u,0} + n\Omega$$

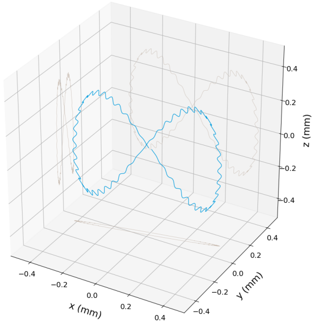


Exemple of an ion's trajectory with $q_z = 0.1$ and $a_z = 0$

# Motion inside a 3D Paul trap

If the stablity condition is met, the solutions have the form :

$$u(\tau) = A \sum_{n=-\infty}^{\infty} c_{2n} \cos\left[(\beta_u + 2n)\,\tau\right] + B \sum_{n=-\infty}^{\infty} c_{2n} \sin\left[(\beta_u + 2n)\,\tau\right]$$

Where $c_{2n}$ depends on $a_u$ and $q_u$

The spectrum of the ion's motion hence contains the frequencies :

$$\omega_{u,n} = (\beta_u + 2n)\,\frac{\omega}{2} = \frac{\beta_u \Omega}{2} + n\Omega = \omega_{u,0} + n\Omega$$

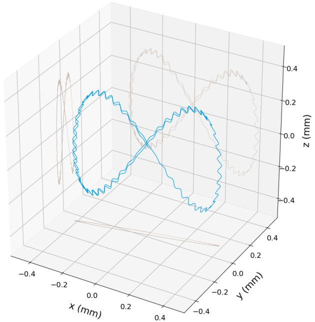


Exemple of an ion's trajectory with $q_z = 0.1$ and $a_z = 0$

# Motion inside a 3D Paul trap

If the stablity condition is met, the solutions have the form :

$$u(\tau) = A \sum_{n=-\infty}^{\infty} c_{2n} \cos\left[(\beta_u + 2n)\,\tau\right] + B \sum_{n=-\infty}^{\infty} c_{2n} \sin\left[(\beta_u + 2n)\,\tau\right]$$

Where $c_{2n}$ depends on $a_u$ and $q_u$

The spectrum of the ion's motion hence contains the frequencies :

$$\omega_{u,n} = (\beta_u + 2n)\,\frac{\omega}{2} = \frac{\beta_u \Omega}{2} + n\Omega = \omega_{u,0} + n\Omega$$

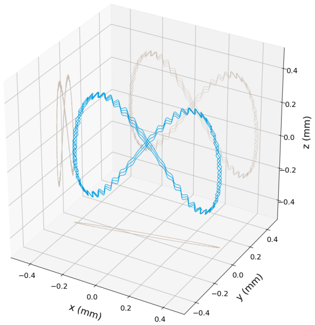


Exemple of an ion's trajectory with $q_z = 0.1$ and $a_z = 0$

# Motion inside a 3D Paul trap

If the stablity condition is met, the solutions have the form :

$$u(\tau) = A \sum_{n=-\infty}^{\infty} c_{2n} \cos\left[(\beta_u + 2n)\,\tau\right] + B \sum_{n=-\infty}^{\infty} c_{2n} \sin\left[(\beta_u + 2n)\,\tau\right]$$

Where $c_{2n}$ depends on $a_u$ and $q_u$

The spectrum of the ion's motion hence contains the frequencies :

$$\omega_{u,n} = (\beta_u + 2n)\,\frac{\omega}{2} = \frac{\beta_u \Omega}{2} + n\Omega = \omega_{u,0} + n\Omega$$

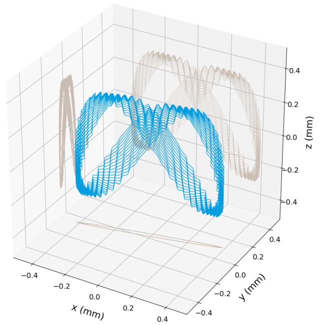


Exemple of an ion's trajectory with $q_z = 0.1$ and $a_z = 0$

# Motion inside a 3D Paul trap

If the stablity condition is met, the solutions have the form :

$$u(\tau) = A \sum_{n=-\infty}^{\infty} c_{2n} \cos\left[(\beta_u + 2n)\,\tau\right] + B \sum_{n=-\infty}^{\infty} c_{2n} \sin\left[(\beta_u + 2n)\,\tau\right]$$

Where $c_{2n}$ depends on $a_u$ and $q_u$

The spectrum of the ion's motion hence contains the frequencies :

$$\omega_{u,n} = (\beta_u + 2n)\,\frac{\omega}{2} = \frac{\beta_u \Omega}{2} + n\Omega = \omega_{u,0} + n\Omega$$

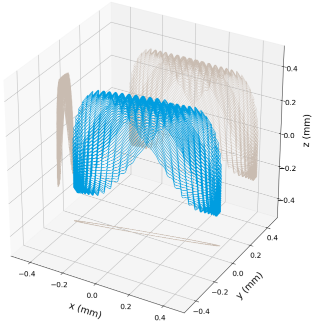


Exemple of an ion's trajectory with $q_z = 0.1$ and $a_z = 0$

# Motion inside a 3D Paul trap

If the stablity condition is met, the solutions have the form :

$$u(\tau) = A \sum_{n=-\infty}^{\infty} c_{2n} \cos\left[(\beta_u + 2n)\,\tau\right] + B \sum_{n=-\infty}^{\infty} c_{2n} \sin\left[(\beta_u + 2n)\,\tau\right]$$

Where $c_{2n}$ depends on $a_u$ and $q_u$

The spectrum of the ion's motion hence contains the frequencies :

$$\omega_{u,n} = (\beta_u + 2n)\,\frac{\omega}{2} = \frac{\beta_u \Omega}{2} + n\Omega = \omega_{u,0} + n\Omega$$

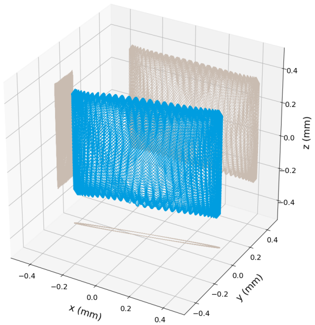


Exemple of an ion's trajectory with $q_z = 0.1$ and $a_z = 0$

# Motion inside a 3D Paul trap

For $a_u$ and $q_u \ll 1$, the $c_{2n}$ coefficient becomes quickly negigible with increasing $n$ and the motion can be viewed as a micromotion at frequency $\Omega$ superimposed on a macromotion at the fundamental frequency $\omega_{u,0} \ll \Omega$

This approximation gets worse and worse as $a_u$ and $q_u$ grows since the higher order components become non-negligible

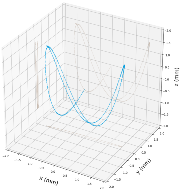


$q_z = 0.02$ and $a_z = 10^{-5}$

# Motion inside a 3D Paul trap

For $a_u$ and $q_u \ll 1$, the $c_{2n}$ coefficient becomes quickly negigible with increasing $n$ and the motion can be viewed as a micromotion at frequency $\Omega$ superimposed on a macromotion at the fundamental frequency $\omega_{u,0} \ll \Omega$

This approximation gets worse and worse as $a_u$ and $q_u$ grows since the higher order components become non-negligible

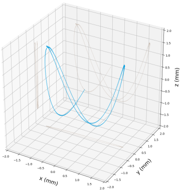


$q_z = 0.02$ and $a_z = 10^{-5}$

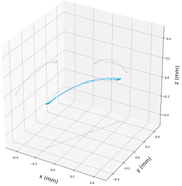


$q_z = 0.2$ and $a_z = 10^{-5}$

# Motion inside a 3D Paul trap

For $a_u$ and $q_u \ll 1$, the $c_{2n}$ coefficient becomes quickly negigible with increasing $n$ and the motion can be viewed as a micromotion at frequency $\Omega$ superimposed on a macromotion at the fundamental frequency $\omega_{u,0} \ll \Omega$

This approximation gets worse and worse as $a_u$ and $q_u$ grows since the higher order components become non-negligible

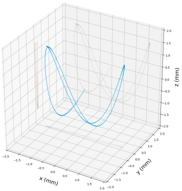


$q_z = 0.02$ and $a_z = 10^{-5}$

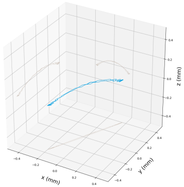


$q_z = 0.2$ and $a_z = 10^{-5}$

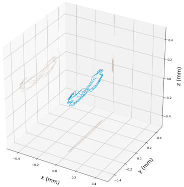


$q_z = 0.4$ and $a_z = 10^{-5}$

# Motion inside a 3D Paul trap

For $a_u$ and $q_u \ll 1$, the $c_{2n}$ coefficient becomes quickly negigible with increasing $n$ and the motion can be viewed as a micromotion at frequency $\Omega$ superimposed on a macromotion at the fundamental frequency $\omega_{u,0} \ll \Omega$

This approximation gets worse and worse as $a_u$ and $q_u$ grows since the higher order components become non-negligible

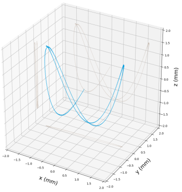


$q_z = 0.02$ and $a_z = 10^{-5}$

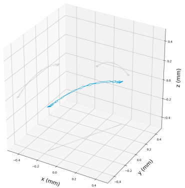


$q_z = 0.2$ and $a_z = 10^{-5}$

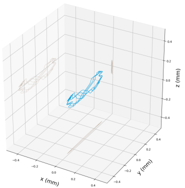


$q_z = 0.4$ and $a_z = 10^{-5}$

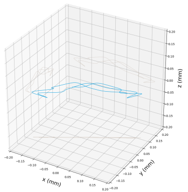


$q_z = 0.6$ and $a_z = 10^{-5}$

# Motion inside a 3D Paul trap

For $a_u$ and $q_u \ll 1$, the $c_{2n}$ coefficient becomes quickly negigible with increasing $n$ and the motion can be viewed as a micromotion at frequency $\Omega$ superimposed on a macromotion at the fundamental frequency $\omega_{u,0} \ll \Omega$

This approximation gets worse and worse as $a_u$ and $q_u$ grows since the higher order components become non-negligible

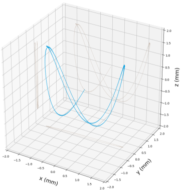

$q_z = 0.02$ and $a_z = 10^{-5}$

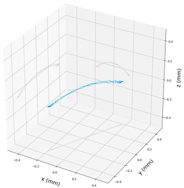

$q_z = 0.2$ and $a_z = 10^{-5}$

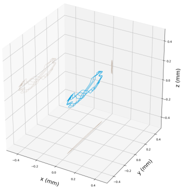

$q_z = 0.4$ and $a_z = 10^{-5}$

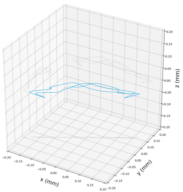

$q_z = 0.6$ and $a_z = 10^{-5}$

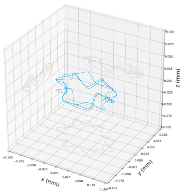

$q_z = 0.8$ and $a_z = 10^{-5}$

# Motion of charged particles in a RF quadrupole trap

Reminder : to have a restoring force proportional to the distance one needs an electric potential :

$$\Phi \propto \lambda x^2 + \mu y^2 + \nu z^2$$

And to obey Laplace's equation, the solution $\lambda = -\mu = +1$ corresponds to a linear Paul trap

In the case of a linear trap (of infinite length), the potential has the form :

$$\Phi = \left[U_{DC} + V_0 \cos(\Omega t)\right] \frac{x^2 - y^2}{2\rho_0^2}$$

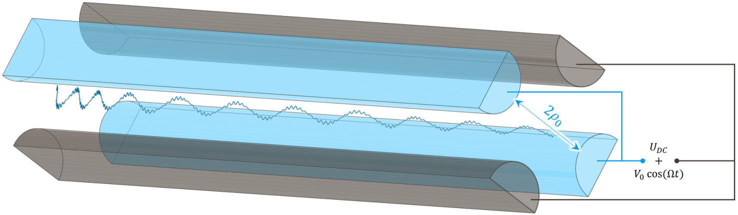

# Stability inside a linear Paul trap

Same kind of reasoning applies to this case so

> Stability of the solution depends on $Q/m$, $\rho_0$, $\Omega$, $U_{DC}$ and $V_0$

with slightly modified expressions of the Mathieu parameters :

$$\begin{cases} a_x = -a_y = \dfrac{4U_{DC}}{\rho_0^2\Omega^2}\dfrac{Q}{m} \\ q_x = -q_y = \dfrac{2V_0}{\rho_0^2\Omega^2}\dfrac{Q}{m} \end{cases}$$

Here the situation is fully symetric for $x$ and $y$ $\Longrightarrow$ the overlap region has a different shape.

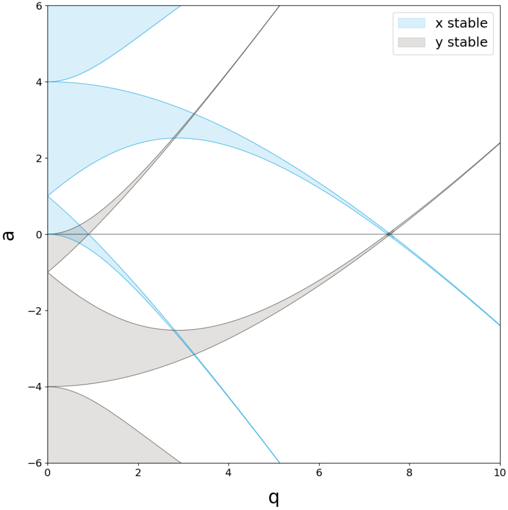

# Stability inside a linear Paul trap

Stability of the solution hence depends on $Q/m$, $\rho_0$, $\Omega$, $U_{DC}$ and $V_0$

Again, mainly the "first" stability region is used

For $a = 0$, the motion is stable for $0 < q \lesssim 0.908$

For a $m = 100$ u ion and a $\rho_0 =$1 cm trap if $U_{DC} = 0$, that means :

- If $V_0 =$100 V, motion is stable for $f = \frac{\Omega}{2\pi} >$183 kHz
- If $f = \frac{\Omega}{2\pi} =$1 MHz, motion is stable for $V_0 <$2,97 kV

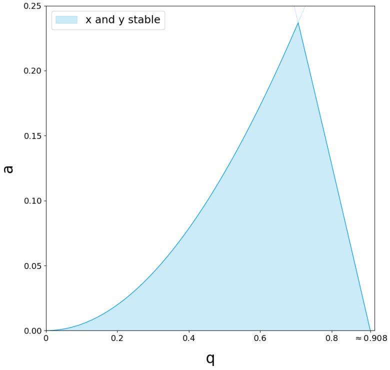

# Cooling with a RF trap

- In nuclear physics, RF quadrupole traps are mainly used for beam cooling and bunching.
- The trap is filled with buffer gas at low pressure ($\sim$ 0,1-1Pa)
- Collisions between the ions and the gas atoms act as a drag force leading to a decrease of the ion's mean velocity

# Cooling with a RF trap

- In nuclear physics, RF quadrupole traps are mainly used for beam cooling and bunching.
- The trap is filled with buffer gas at low pressure ($\sim$ 0,1-1Pa)
- Collisions between the ions and the gas atoms act as a drag force leading to a decrease of the ion's mean velocity

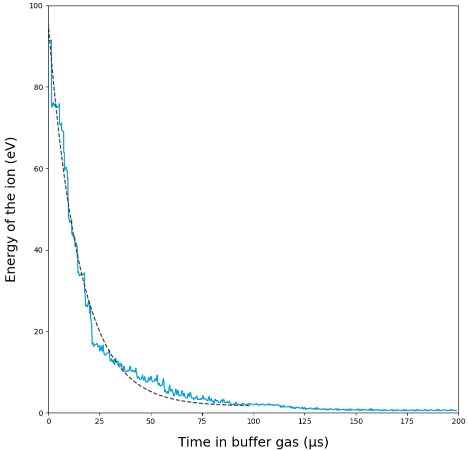


Kinetic energy of an $A = 100$ ion in 1 Pa of He

# Cooling with a RF trap

- In nuclear physics, RF quadrupole traps are mainly used for beam cooling and bunching.
- The trap is filled with buffer gas at low pressure ($\sim$ 0,1-1Pa)
- Collisions between the ions and the gas atoms act as a drag force leading to a decrease of the ion's mean velocity
- An axial DC potential ramp keep the ion moving towards the exit of the RFQ

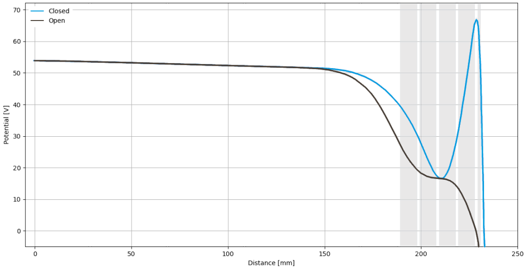

# Cooling with a RF trap

- In nuclear physics, RF quadrupole traps are mainly used for beam cooling and bunching.
- The trap is filled with buffer gas at low pressure ($\sim$ 0,1-1Pa)
- Collisions between the ions and the gas atoms act as a drag force leading to a decrease of the ion's mean velocity
- An axial DC potential ramp keep the ion moving towards the exit of the RFQ
- This results in a lower transverse emittance

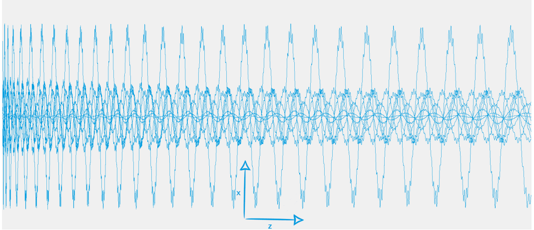


10 ions, $q = 0.2$ , $a = 0$ and no gas

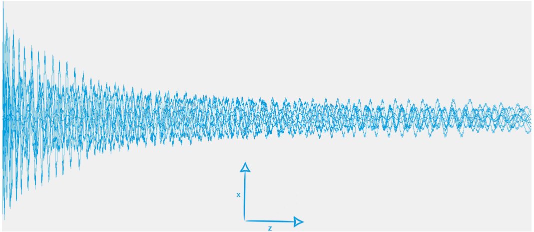


10 ions, $q = 0.2$ , $a = 0$ and $P_{He}$ =1 Pa

# Cooling with a RF trap

Example : cooling of a 30 keV beam of $^{40}K$ in shoot-through mode in a 90 cm-long RFQ filled with $\approx$ 1 Pa of He at room temperature.

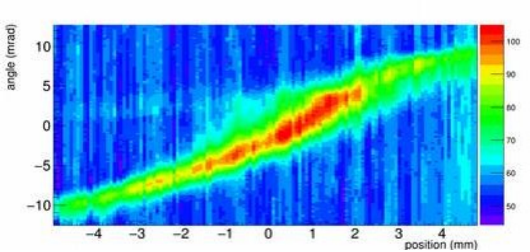


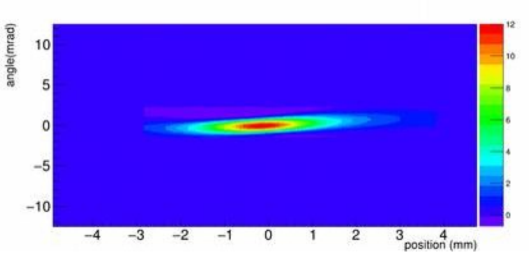


Before

$\epsilon_{(95\%)} = 18\pi$ mm mrad

After

$\epsilon_{(95\%)} = 3\pi$ mm mrad

# Bunching with a RF trap

Once cooled the ions can either...

- be extracted from the RFQ continuously (CW beam).
- be trapped in a potential well at the end of the RFQ and released periodically (bunched beam)

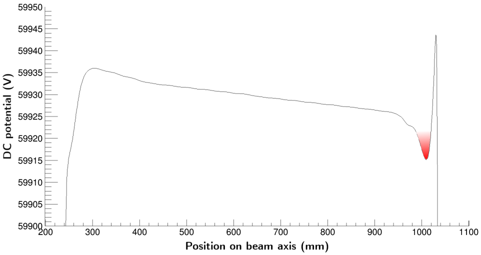


simulations by H. Guérin

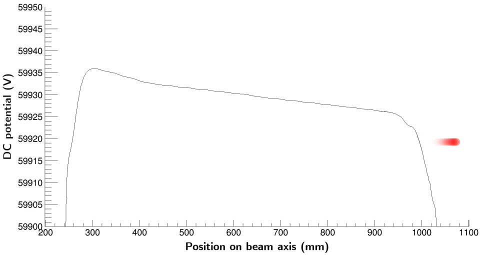

# Some examples of RFQCB - ISCOOL & GPIB

- $\rho_0 = 20\,\mathrm{mm}$ , $V_0$ up to $4\,\mathrm{kV}$
- RF is fed to 4 rods
- DC gradient is provided by 25 annular electrodes with wedges towards the axis

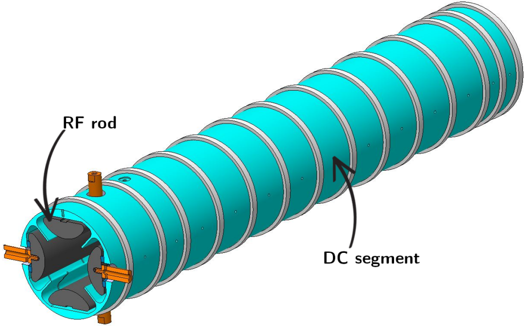


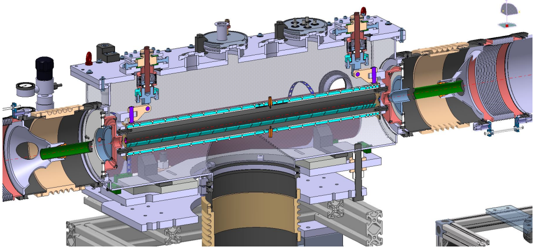

# Some examples of RFQCB - SHIRaC2

- Aims at cooling up to 1 μA of 1+ ions from 80 to 2 $\pi$ mm mrad
- $\rho_0 = 5\,\text{mm}$ , $V_0$ up to 8 kV
- The 4 rods are segmented into 18 segments
- RF and DC are coupled for each segment to create a DC gradient

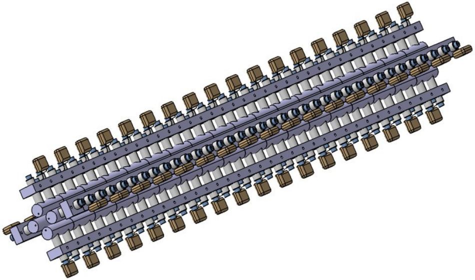

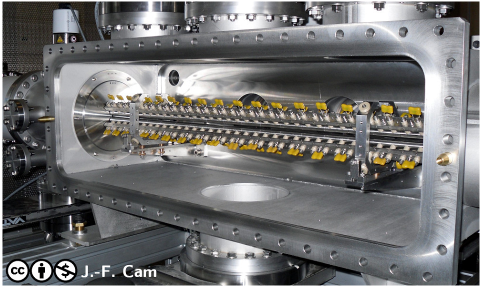

# Some examples of RFQCB - LEBIT ion cooler and buncher

- $\rho_0 = 13{,}5\,\text{mm}$ , $V_0 \sim 1\,\text{kV}$
- RF is fed to 4 rods
- Drag potential created by segmenting diagonally an outer cylindrical electrode into 2 pairs
- Fraction of each electrode pair visible from the inner part varies along the axis

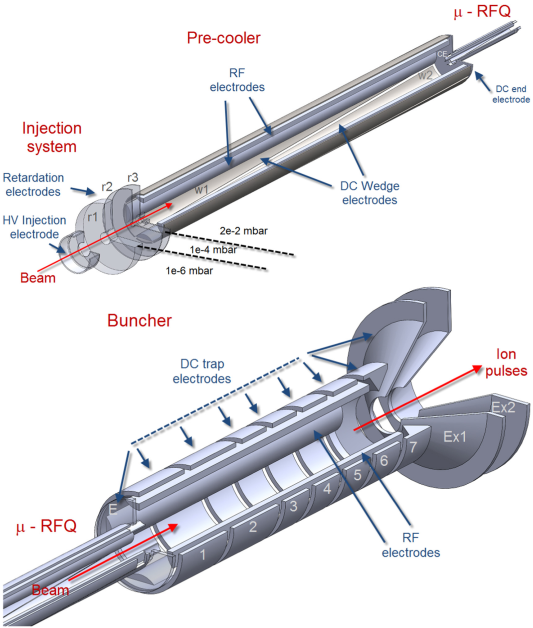


Figures from S. Schwarz *et al*, Nucl. Inst. Meth. 816,131 (2016)

# Penning traps

# The Penning way of trapping

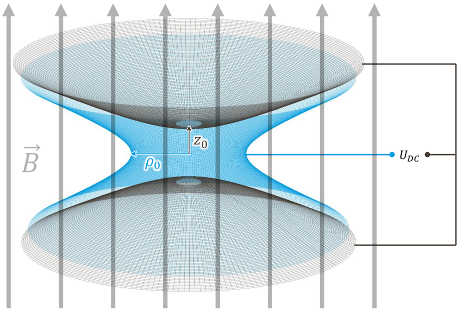


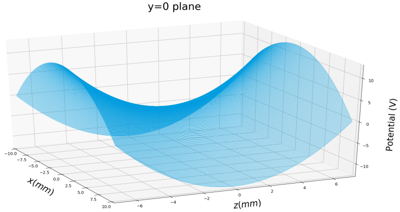


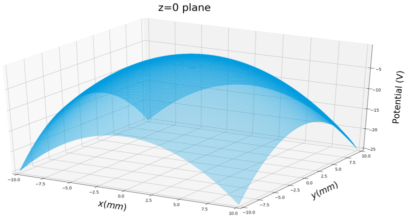


Static quadrupole potential

# Motion of a charged particle in a Penning trap

- The axial motion is confined by the quadrupolar electric potential

$$\Phi = U_{DC}\frac{-x^2 - y^2 + 2z^2}{4d_0^2}$$

- For a particle with mass $m$ and charge $Q$ on the trap axis with no transverse velocity, the motion is a simple harmonic oscillation at angular frequency $\omega_z$

$$\omega_z = \sqrt{\frac{QU_{DC}}{md_0^2}}$$

- The radial motion is confined by the homogeneous magnetic field $B$
- If there was no electric field, the charged particle would simply have a circular motion at the cyclotron angular frequency $\omega_c$

**Cyclotron angular frequency**

$$\omega_c = \frac{QB}{m}$$

# Motion of a charged particle in a Penning trap

When combining both fields, the force applied to the charge particle is :

$$\vec{F} = Q\left(-\vec{\nabla}\Phi + \vec{v} \times \vec{B}\right)$$

The equations of motion of the particle are then :

$$\begin{cases} \ddot{x} = \omega_c \dot{y} + \dfrac{\omega_z^2}{2} x \\ \ddot{y} = -\omega_c \dot{x} + \dfrac{\omega_z^2}{2} y \\ \ddot{z} = -\omega_z^2 z \end{cases}$$

simple harmonic oscillator

# Motion of a charged particle in a Penning trap

When combining both fields, the force applied to the charge particle is :

$$\vec{F} = Q\left(-\vec{\nabla}\Phi + \vec{v} \times \vec{B}\right)$$

The equations of motion of the particle are then :

$$\begin{cases} \ddot{x} = \omega_c \dot{y} + \frac{\omega_z^2}{2} x \\ \ddot{y} = -\omega_c \dot{x} + \frac{\omega_z^2}{2} y \\ \ddot{z} = -\omega_z^2 z \end{cases} \iff \begin{cases} u = x + iy \\ \ddot{u} = -i\omega_c \dot{x} + \frac{\omega_z^2}{2} u \\ \ddot{z} = -\omega_z^2 z \end{cases}$$

simple harmonic oscillator

# Motion of a charged particle in a Penning trap

When combining both fields, the force applied to the charge particle is :

$$\vec{F} = Q\left(-\vec{\nabla}\Phi + \vec{v} \times \vec{B}\right)$$

The equations of motion of the particle are then :

$$\begin{cases} \ddot{x} = \omega_c \dot{y} + \frac{\omega_z^2}{2} x \\ \ddot{y} = -\omega_c \dot{x} + \frac{\omega_z^2}{2} y \\ \ddot{z} = -\omega_z^2 z \end{cases} \iff \begin{cases} u = x + iy \\ \ddot{u} = -i\omega_c \dot{x} + \frac{\omega_z^2}{2} u \\ \ddot{z} = -\omega_z^2 z \end{cases}$$

simple harmonic oscillator

For the radial part, looking for solutions of the form : $u \propto e^{-i\omega t}$, one finds : $\omega^2 - \omega_c \omega - \frac{\omega_z^2}{2} = 0$

The eigenfrequencies are then : $\omega_\pm = \frac{\omega_c \pm \sqrt{\omega_c^2 - 2\omega_z^2}}{2} = \frac{\omega_c}{2} \pm \sqrt{\frac{\omega_c^2}{4} - \frac{\omega_z^2}{2}}$

# Eigenmotions - what it looks like

The motion is the compound of 3 eigenmotions with angular frequencies :

- $\omega_z$ (axial motion) : harmonic oscillation between endcaps
- $\omega_+$ (modified cyclotron motion) : around $B$ field lines
- $\omega_-$ (magnetron motion) : much slower $\vec{E} \times \vec{B}$ drift around trap center

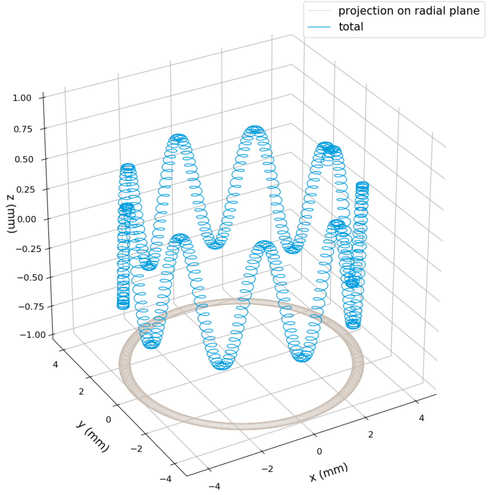


(unrealistic ratio between the eigenfrequencies)

# Eigenmotions - what it looks like

The motion is the compound of 3 eigenmotions with angular frequencies :

- $\omega_z$ (axial motion) : harmonic oscillation between endcaps
- $\omega_+$ (modified cyclotron motion) : around $B$ field lines
- $\omega_-$ (magnetron motion) : much slower $\vec{E} \times \vec{B}$ drift around trap center

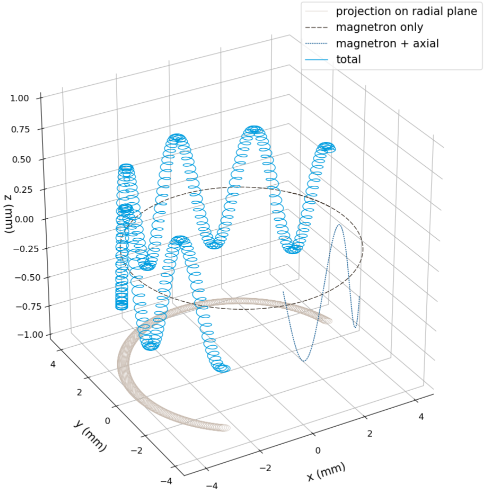

# Eigenmotions - what it looks like

The motion is the compound of 3 eigenmotions with angular frequencies :

- $\omega_z$ (axial motion) : harmonic oscillation between endcaps
- $\omega_+$ (modified cyclotron motion) : around $B$ field lines
- $\omega_-$ (magnetron motion) : much slower $\vec{E} \times \vec{B}$ drift around trap center

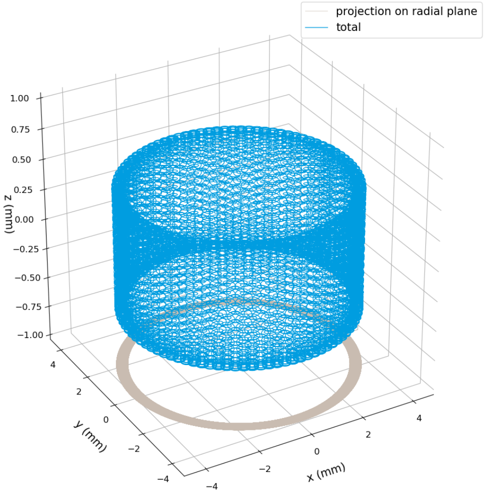


(realistic ratio between the eigenfrequencies)

# Eigenfrequencies

These angular frequencies are linked by :

$$\omega_+ + \omega_- = \omega_c$$

And also

**Invariance theorem**

$$\omega_+^2 + \omega_-^2 + \omega_z^2 = \omega_c^2$$

And the ion motion is stable only if :

**Trap stability condition**

$$\omega_+ > \omega_- \iff \omega_c > \sqrt{2}\omega_z$$

Usually, $\omega_c \sim \omega_+ \gg \omega_z \gg \omega_-$

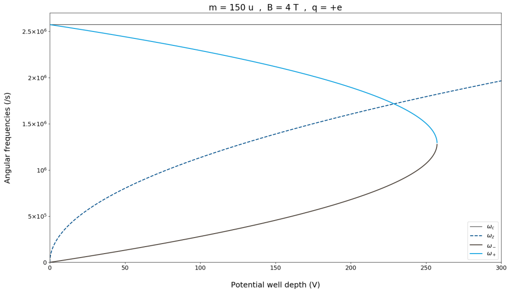


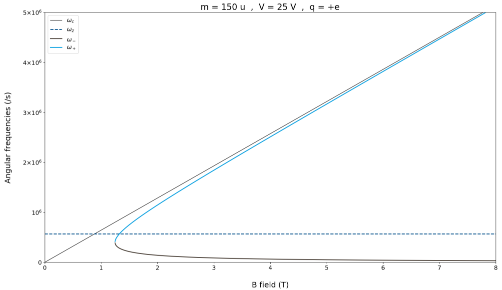

# How it looks like in practice

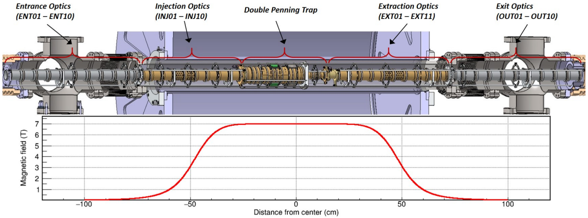


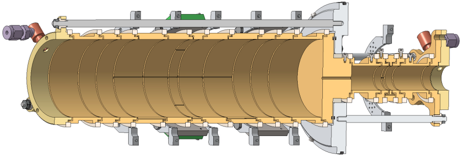

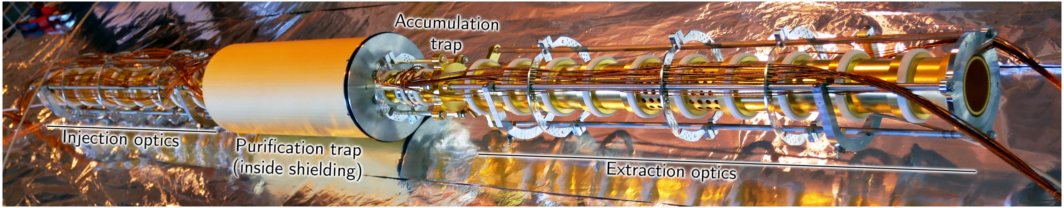


Strong and very homogeneous magnetic field $\Longrightarrow$ costly and cryogenic + care for materials needed

# Penning trap techniques

"Never measure anything but frequency !"
(Arthur L. Schawlow)

# Playing with the eigenmotions - quantum point of view

- We have studied the motion in a classical way but it can be of course be treated fully quantum mechanically
- Noteworthy : negative energy for the magnetron motion
- Each of the eigenmotions can be individually manipulated by applying a resonant RF excitation at the corresponding eigenfrequency

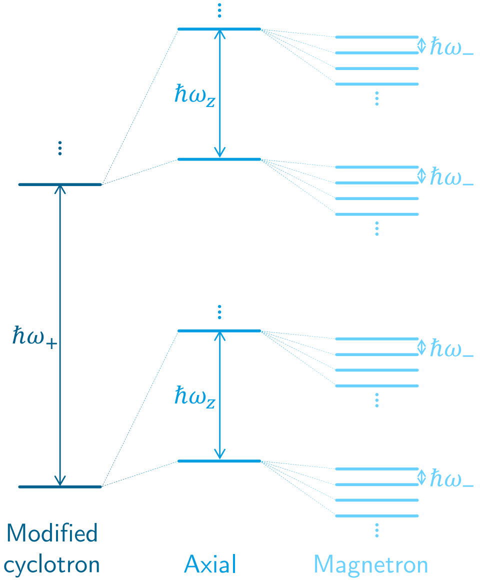

# RF excitation

For the radial motions, this requires segmentation of the electrodes

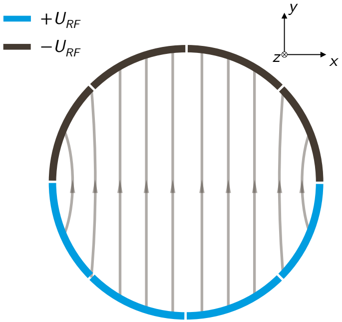


Dipole excitation

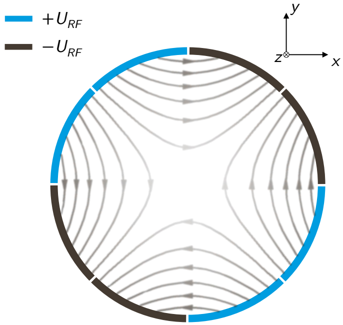


Quadrupole excitation

# RF excitation

For the radial motions, this requires segmentation of the electrodes

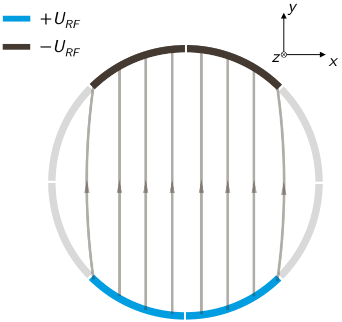


Dipole excitation

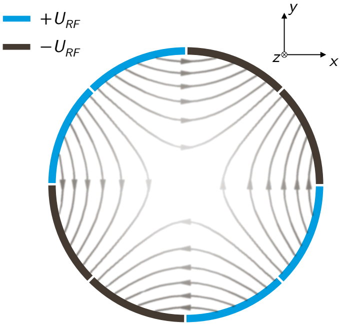


Quadrupole excitation

# Amplifying the magnetron motion

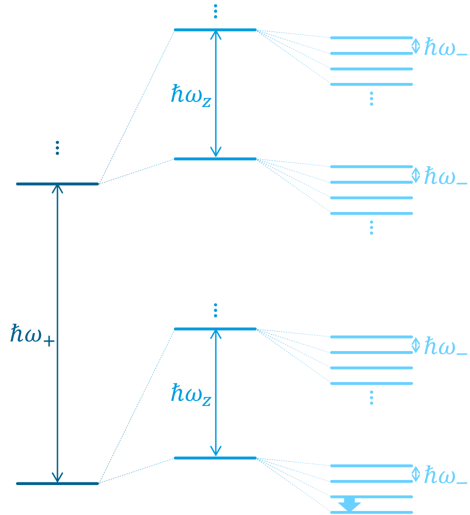


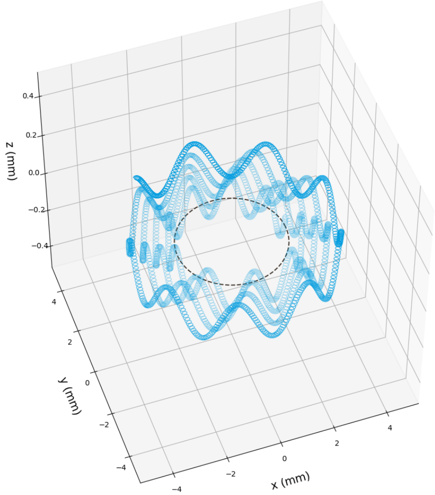


Dipole excitation at $\omega = \omega_-$

(not mass selective !)

# Amplifying the magnetron motion

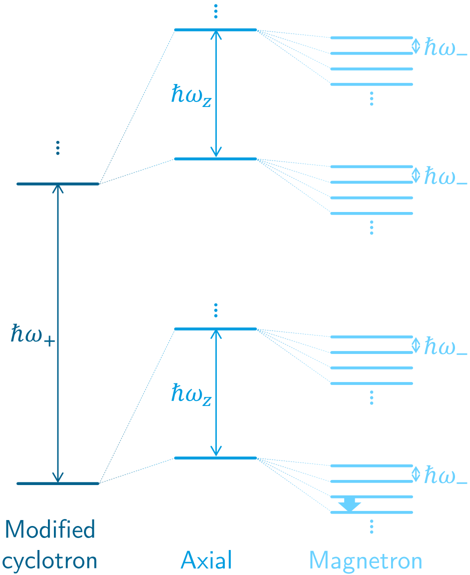


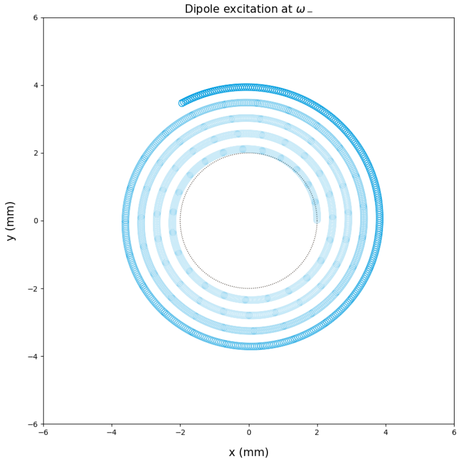


Dipole excitation at $\omega = \omega_-$

(not mass selective !)

# Amplifying the axial motion

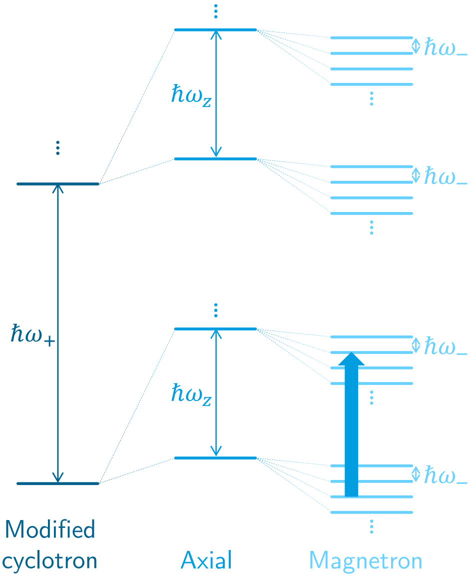


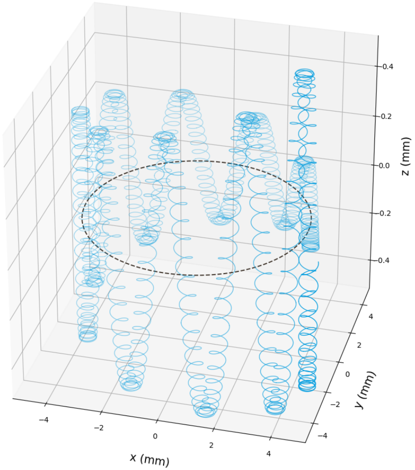


Dipole excitation at $\omega = \omega_z$

(mass selective)

# Amplifying the axial motion

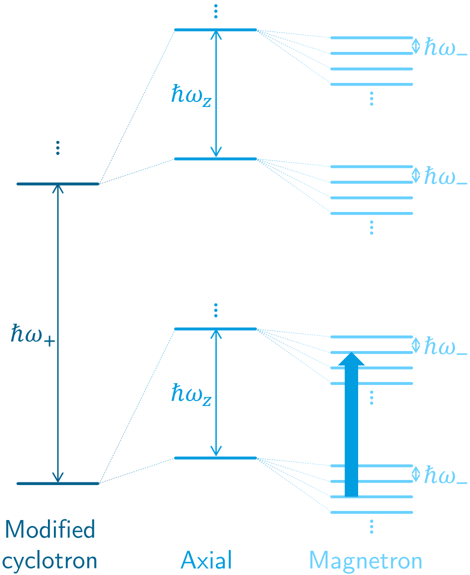


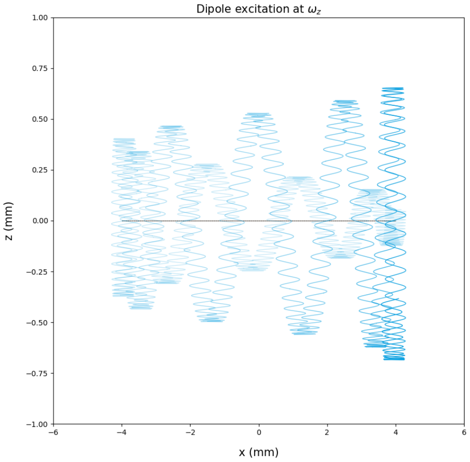


Dipole excitation at $\omega = \omega_z$

(mass selective)

# Amplifying the modified cyclotron motion

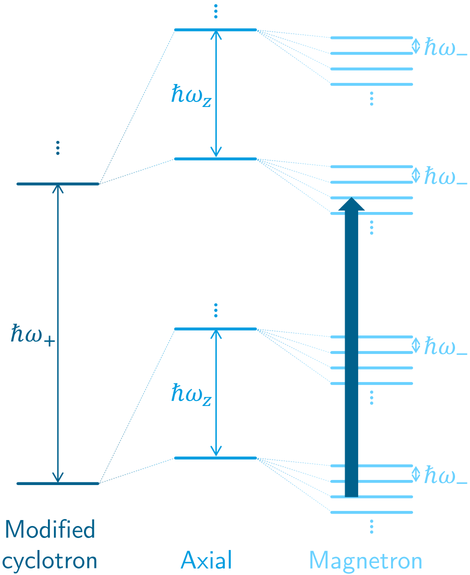


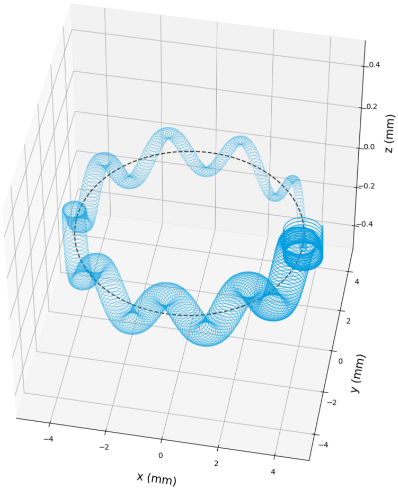


Dipole excitation at $\omega = \omega_+$

(mass selective)

# Amplifying the modified cyclotron motion

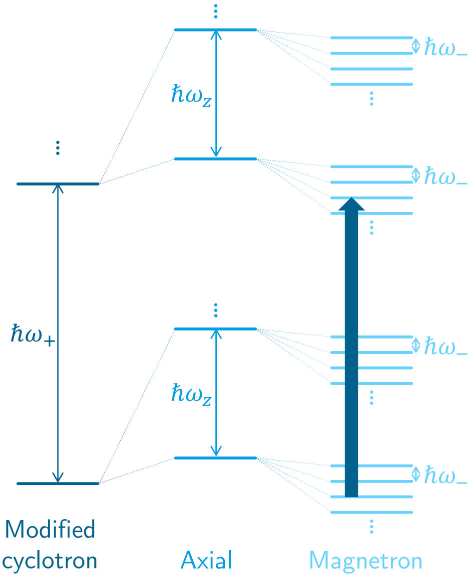


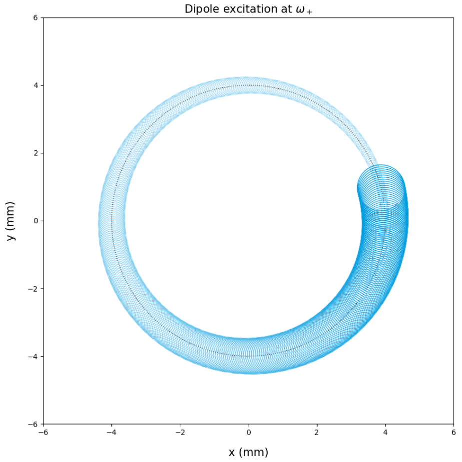


Dipole excitation at $\omega = \omega_+$

(mass selective)

# Converting one motion into another

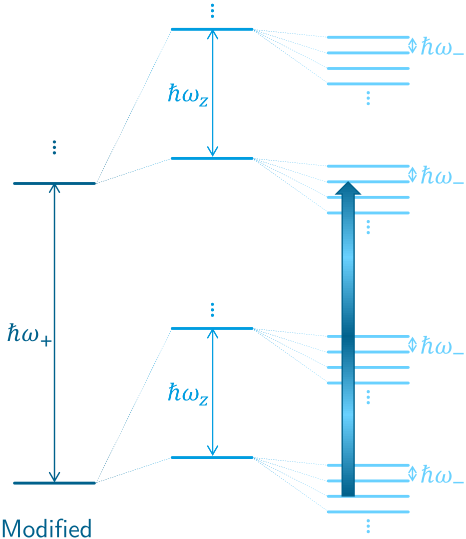


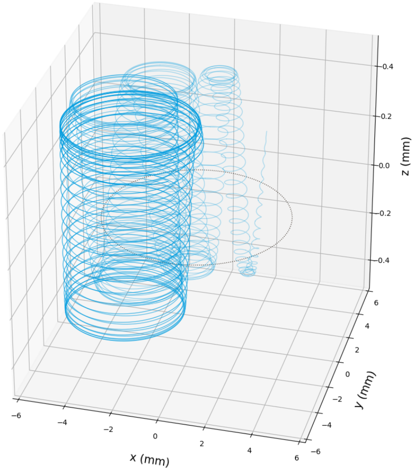


Quadrupole excitation at $\omega = \omega_c$

(mass selective)

# Converting one motion into another

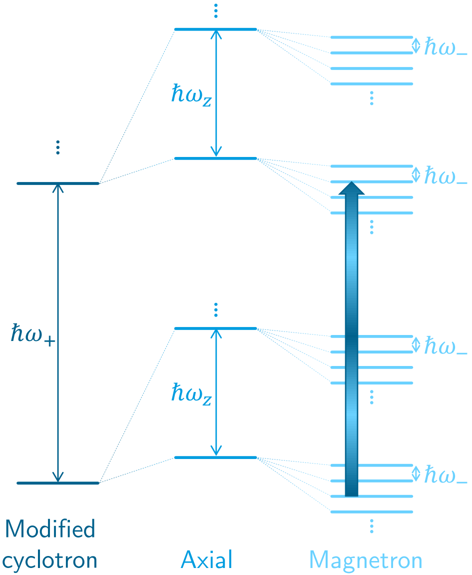


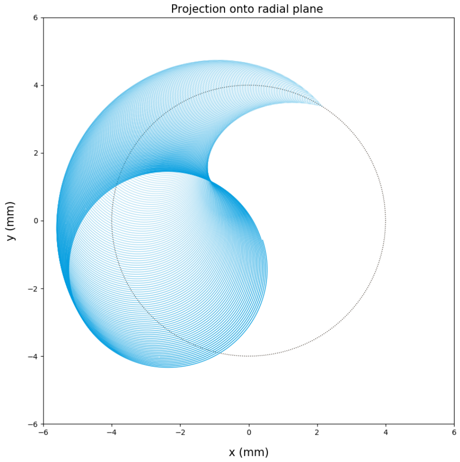


Quadrupole excitation at $\omega = \omega_c$

(mass selective)

# Converting one motion into another

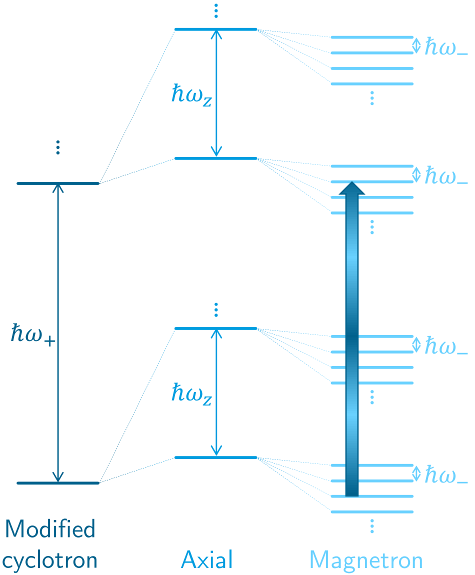


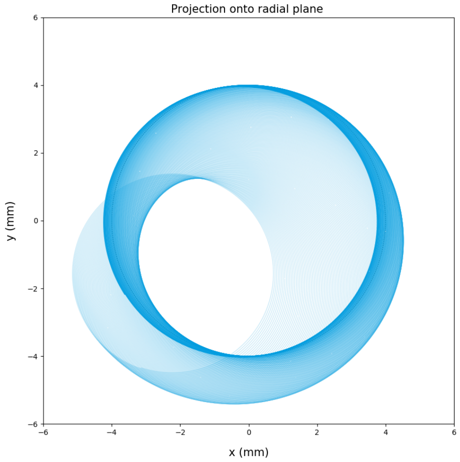


Quadrupole excitation at $\omega = \omega_c$

(mass selective)

# Converting one motion into another

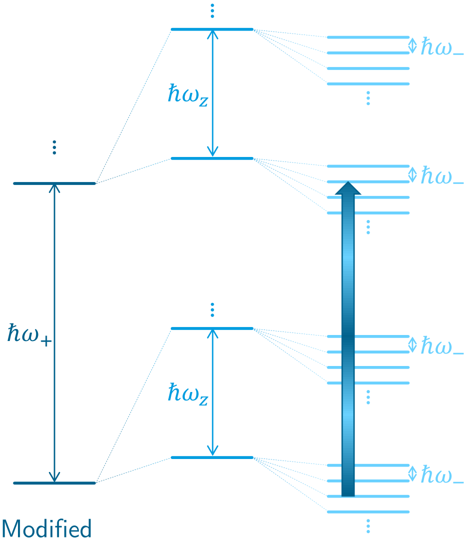


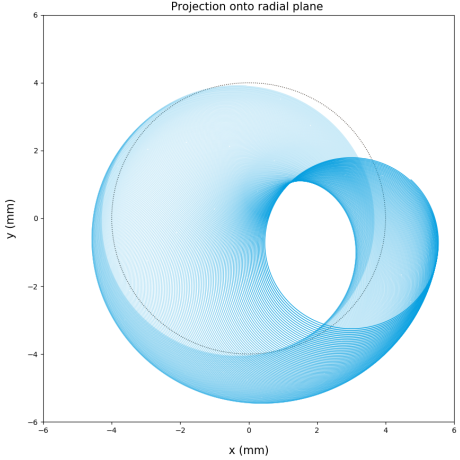


Quadrupole excitation at $\omega = \omega_c$

(mass selective)

# Converting one motion into another

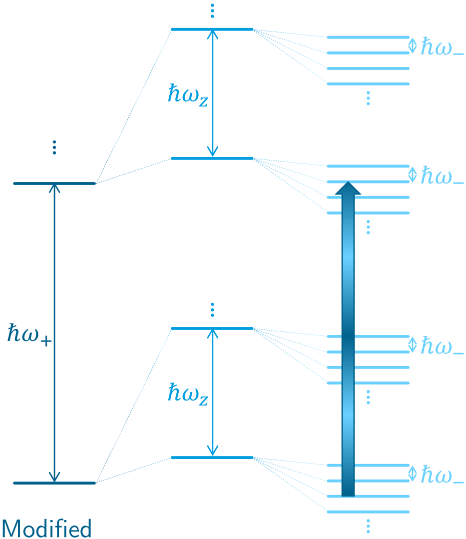


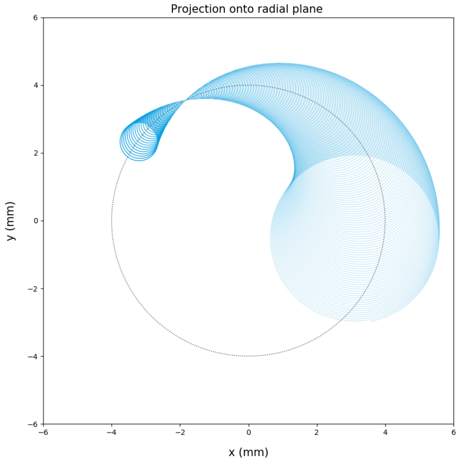


Quadrupole excitation at $\omega = \omega_c$

(mass selective)

# Converting one motion into another

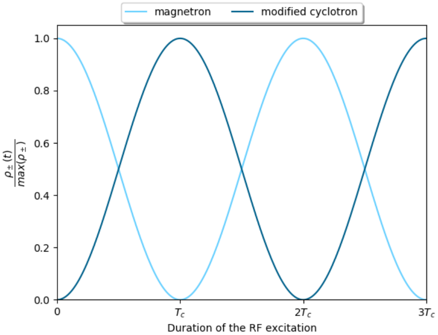


Time needed for one full conversion :

$$T_c = \frac{\omega_+ - \omega_-}{u_{RF}} \rho_-^2 \frac{m}{Q} \approx \frac{B_0}{u_{RF}} \rho_-^2$$

with $B_0 = 7\,\mathrm{T}$, $u_{RF} = 10\,\mathrm{mV}$ and $\rho_-(0) = 1\,\mathrm{mm}$, $T_c = 700\,\mu\mathrm{s}$

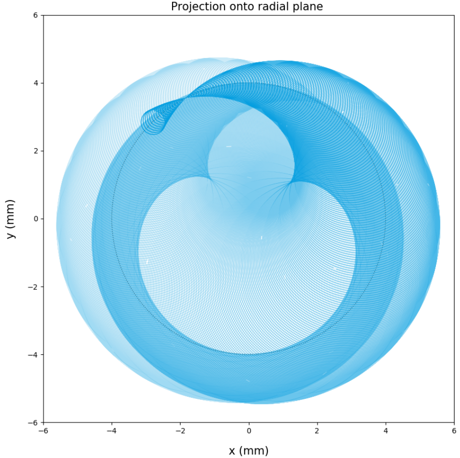


Quadrupole excitation at $\omega = \omega_c$

(mass selective)

# Converting one motion into another

- If the excitation is not made exactly at the right frequency, the conversion efficiency is decreased

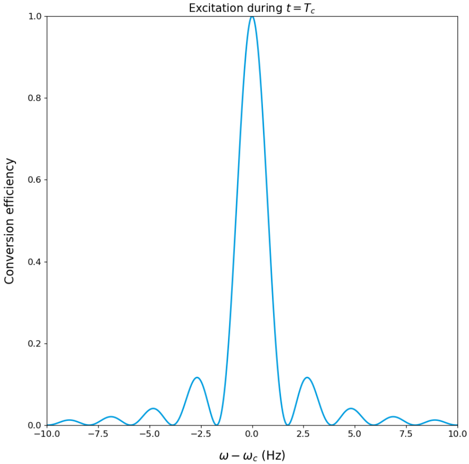

# Converting one motion into another

- If the excitation is not made exactly at the right frequency, the conversion efficiency is decreased
- The longer the excitation, the narrower is the resonance

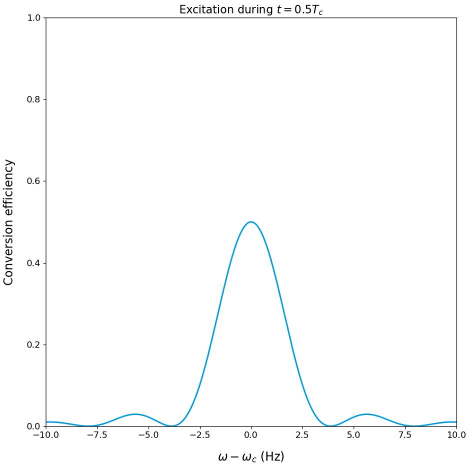

# Converting one motion into another

- If the excitation is not made exactly at the right frequency, the conversion efficiency is decreased
- The longer the excitation, the narrower is the resonance

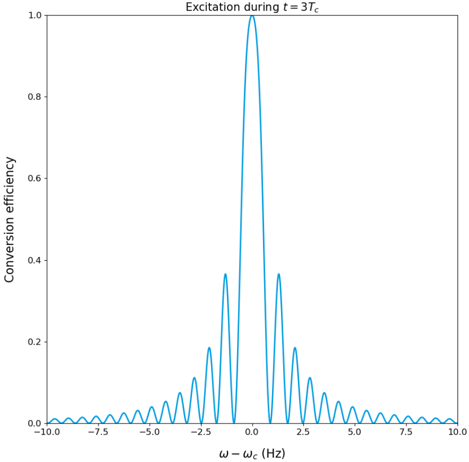

# Damping the motions

The motions can be damped in different ways (resistive, sympathetic, laser cooling,...) but for radioactive ions buffer gas cooling is generally used

- A buffer gas at low pressure ($\sim 10^{-3}$Pa) is injected in the trap
- The ions lose energy through the collisions with the gas

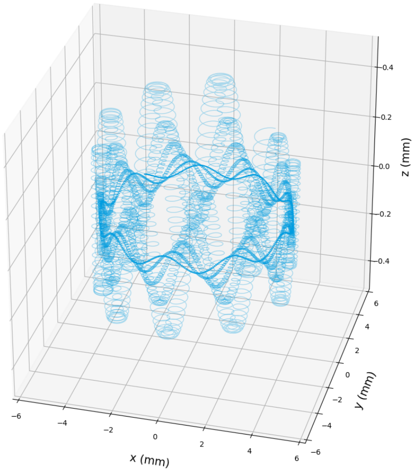

# Buffer gas cooling with modified cyclotron or axial motion

- Both axial and modified cyclotron motions are damped when the ions collide with the buffer gas $\Rightarrow \rho_i = \rho_{0,i} \exp^{-\alpha_i t}$
- The damping rate depends linearly on the gas pressure and inversely on the ion mobility

$$\alpha_\pm = \pm \frac{Q}{m} \frac{1}{\mu_{ion}} \frac{pT_N}{p_N T} \frac{\omega_\pm}{\omega_+ - \omega_-} \qquad \alpha_z = \frac{Q}{m} \frac{1}{\mu_{ion}} \frac{pT_N}{p_N T}$$

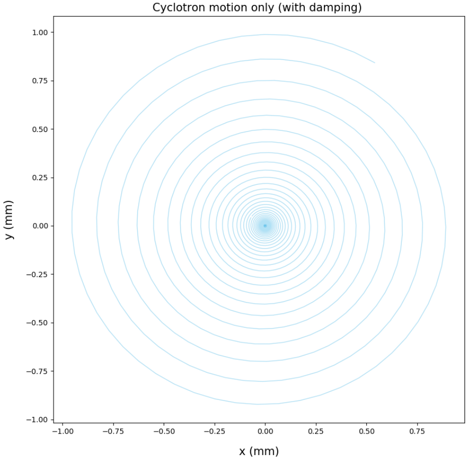

# Buffer gas cooling with magnetron motion

- On the contrary, the magnetron motion is slowly amplified by the collisions with the gas
- This is due to the negative energy of the magnetron motion

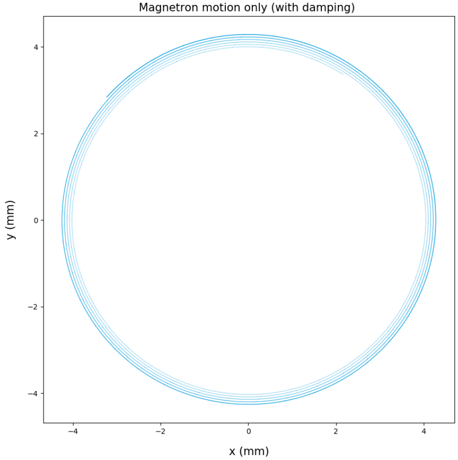

# Axialisation

- All three motions of a given species can be damped at once by coupling buffer gas colling with a quadrupolar excitation at $\omega_c$
- This is hence mass selective

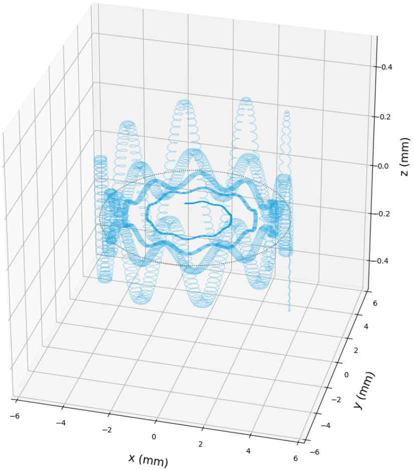

# Axialisation

- All three motions of a given species can be damped at once by coupling buffer gas colling with a quadrupolar excitation at $\omega_c$
- This is hence mass selective

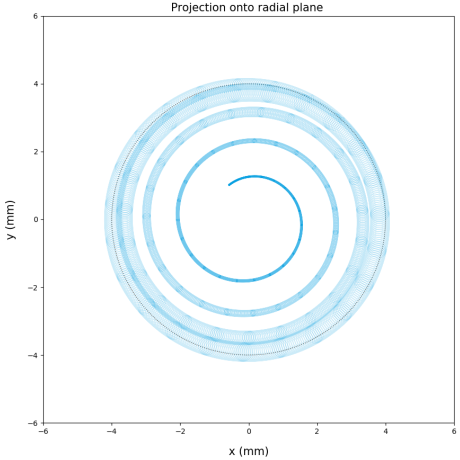

# ToF-ICR

- If the ion has a non-zero radial velocity, it also has an associated magnetic moment $\vec{\mu} = \frac{Q\omega r^2}{2\pi}\vec{e}_z$
- This corresponds to a radial energy $\mathcal{E} = -\vec{\mu} \cdot \vec{B}$
- When ejected toward a detector, ions travel through the $\vec{B}$ field gradient and are accelerated by a force $\vec{F} = -\vec{\nabla}\mathcal{E}_p = \vec{\nabla}\left(\vec{\mu} \cdot \vec{B}\right)$
- For a given radius of the trajectory inside the trap, the accelerating force will hence be higher for a modified cyclotron motion than for a magnetron one

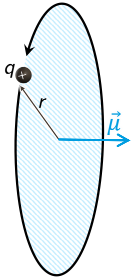

# ToF-ICR

The time of flight of a particle of charge $Q$ to a detector outside the magnet is given by :

$$T_f = \sqrt{\frac{m}{2}} \int_{z_0}^{z_{det}} \frac{dz}{\sqrt{\mathcal{E}_0 - QV(z) - \mu B(z)}}$$

where $\mathcal{E}_0$ is the total kinetic energy of the ion, $V(z)$ the electric potential

# ToF-ICR

The time of flight of a particle of charge $Q$ to a detector outside the magnet is given by :

$$T_f = \sqrt{\frac{m}{2}} \int_{z_0}^{z_{det}} \frac{dz}{\sqrt{\mathcal{E}_0 - QV(z) - \mu B(z)}}$$

where $\mathcal{E}_0$ is the total kinetic energy of the ion, $V(z)$ the electric potential

ToF-ICR method : apply a quadrupolar excitation at different $\omega$ to ions with some magnetron motion

> The better the conversion from magnetron to cyclotron, the shorter the time of flight
>
> $\Rightarrow T_f = f(\omega)$ has a dip at $\omega_c$

The mass of the ion is then $m = \frac{QB}{\omega_c}$

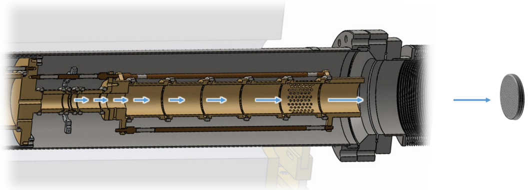

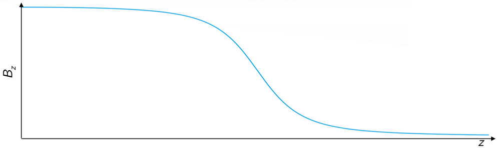


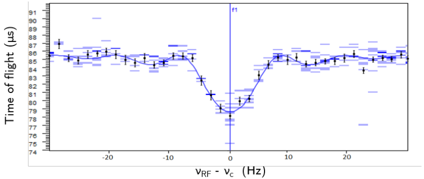


ToF of $^{115}$Ru ions at JYFLTRAP (100ms)

# ToF-ICR

As the measured quantity is the cyclotron frequency...

You never know the mass at a relative precision better than the one of the magnetic field !

⇒ $B$ field measurement mandatory at each "mass" measurement

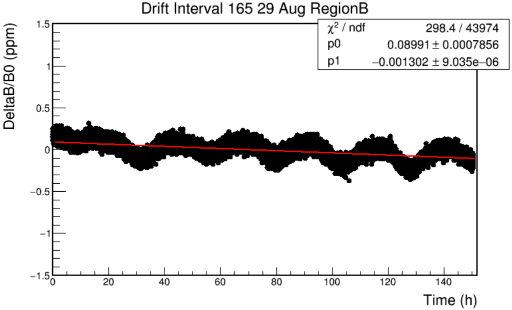


The $\omega_c$ of a "reference" ion (of well known mass) must be measured before and after an unknown mass measurement

# ToF-ICR

As the measured quantity is the cyclotron frequency...

You never know the mass at a relative precision better than the one of the magnetic field !

$\Rightarrow$ $B$ field measurement mandatory at each "mass" measurement

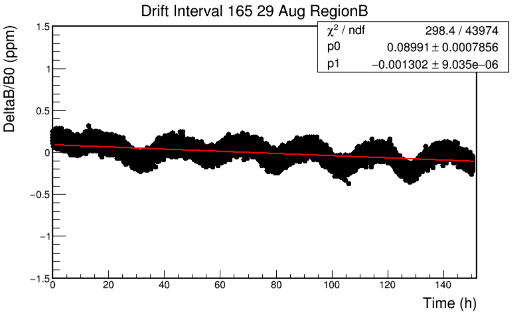


The $\omega_c$ of a "reference" ion (of well known mass) must be measured before and after an unknown mass measurement

Other things to be carefully taken into account : misalignment, tilt, machining imperfetions, high order components for the fields ($>$2 for $\vec{E}$, $>$0 for $\vec{B}$), space charge effects, ...

# Ramsey time-separated oscillatory fields

ToF-ICR has been the workhorse of nuclear mass-measurements for more than 30 years but several other methods have been developed to boost the precision

- In Ramsey's method, the RF excitation is split in 2 (or more) pulses with a waiting period in between

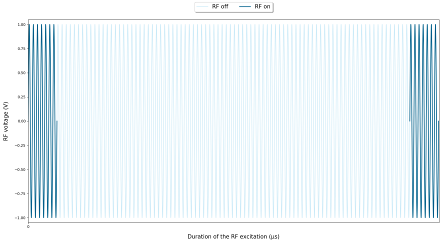

# Ramsey time-separated oscillatory fields

ToF-ICR has been the workhorse of nuclear mass-measurements for more than 30 years but several other methods have been developed to boost the precision

- In Ramsey's method, the RF excitation is split in 2 (or more) pulses with a waiting period in between
- This results in sharper resonance
- The waiting period needs to be (significantly) longer than the 2 pulses to get a real benefit

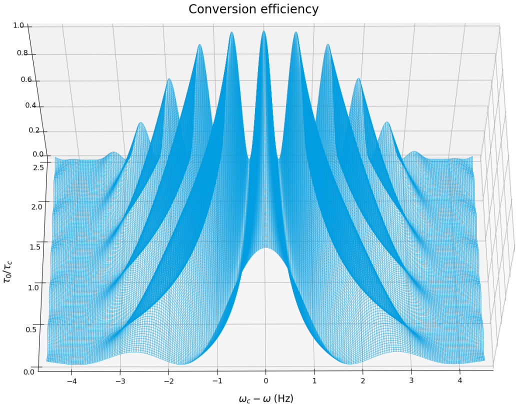

# Ramsey time-separated oscillatory fields

ToF-ICR has been the workhorse of nuclear mass-measurements for more than 30 years but several other methods have been developed to boost the precision

- In Ramsey's method, the RF excitation is split in 2 (or more) pulses with a waiting period in between
- This results in sharper resonance
- The waiting period needs to be (significantly) longer than the 2 pulses to get a real benefit

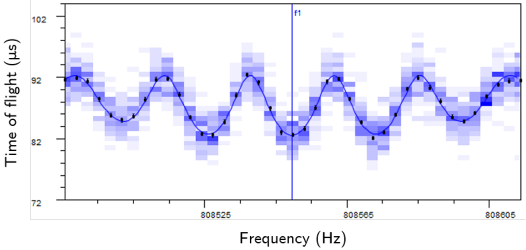


Ramsey ToF of $^{133}$Cs ions at JYFLTRAP (10ms-30ms-10ms)

# Phase-imaging ion-cyclotron-resonance

- The most precise mass-measurement method to date is the PI-ICR technique
- Independent measurement of $\omega_-$ and $\omega_+$ by preparing the ions in a pure magnetron or modified cyclotron state, letting them evolve freely during an accumulation time and then extracting them towards the detector
- Requires a position-sensitive detector ! (delay-line MCP)

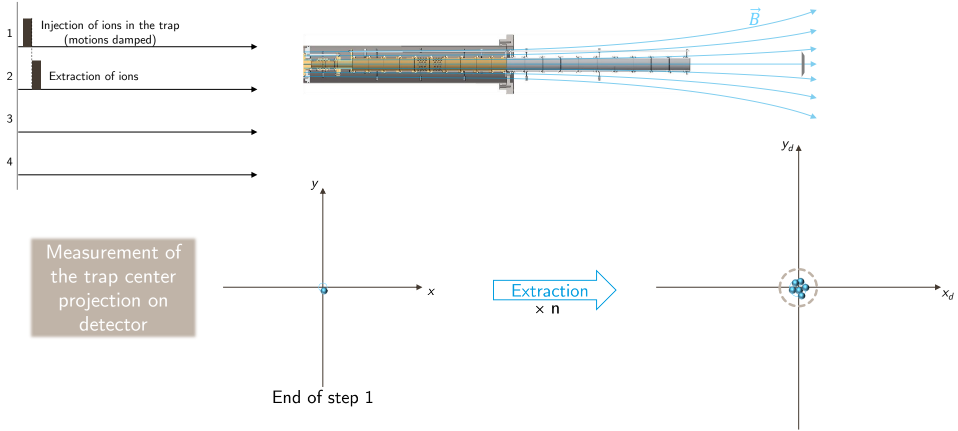

# Phase-imaging ion-cyclotron-resonance

- The most precise mass-measurement method to date is the PI-ICR technique
- Independent measurement of $\omega_-$ and $\omega_+$ by preparing the ions in a pure magnetron or modified cyclotron state, letting them evolve freely during an accumulation time and then extracting them towards the detector
- Requires a position-sensitive detector ! (delay-line MCP)

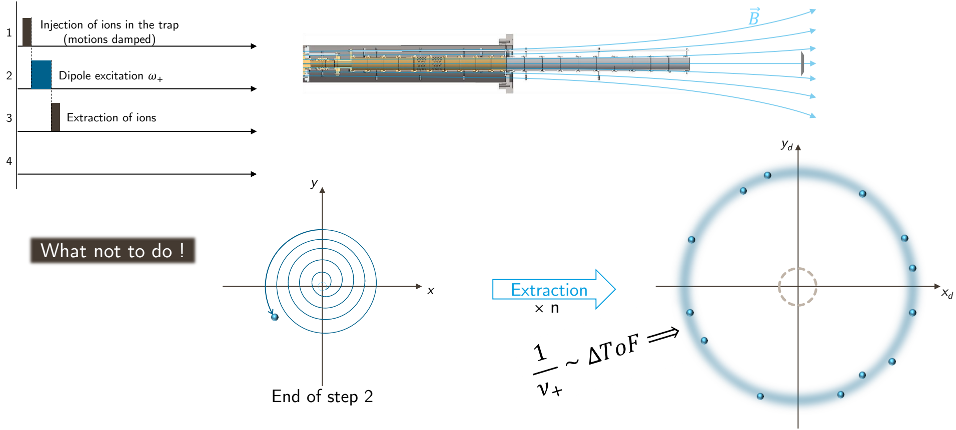

# Phase-imaging ion-cyclotron-resonance

- The most precise mass-measurement method to date is the PI-ICR technique
- Independent measurement of $\omega_-$ and $\omega_+$ by preparing the ions in a pure magnetron or modified cyclotron state, letting them evolve freely during an accumulation time and then extracting them towards the detector
- Requires a position-sensitive detector ! (delay-line MCP)

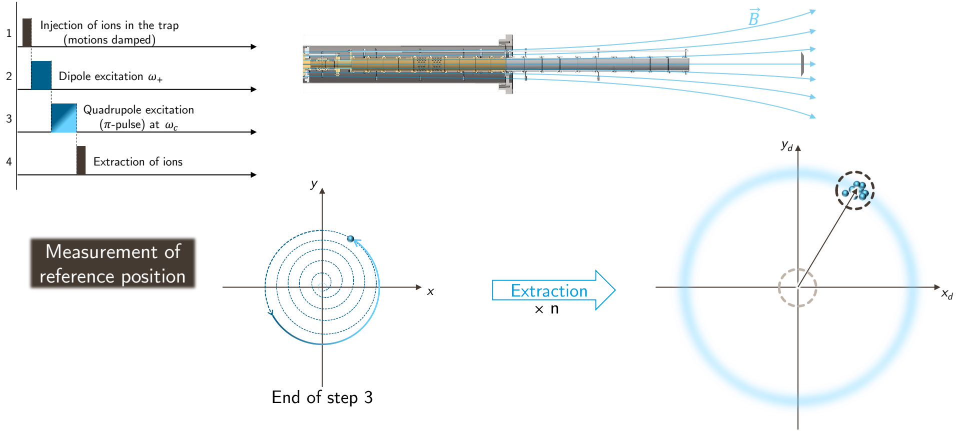

# Phase-imaging ion-cyclotron-resonance

- The most precise mass-measurement method to date is the PI-ICR technique
- Independent measurement of $\omega_-$ and $\omega_+$ by preparing the ions in a pure magnetron or modified cyclotron state, letting them evolve freely during an accumulation time and then extracting them towards the detector
- Requires a position-sensitive detector ! (delay-line MCP)

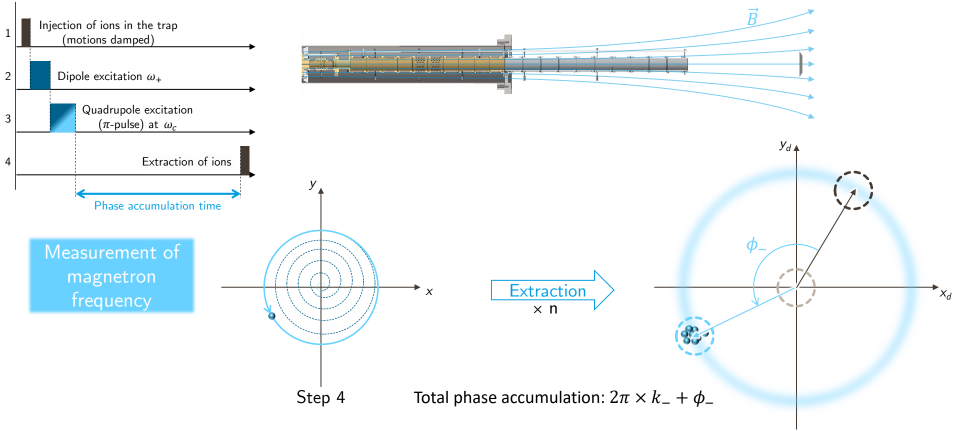

# Phase-imaging ion-cyclotron-resonance

- The most precise mass-measurement method to date is the PI-ICR technique
- Independent measurement of $\omega_-$ and $\omega_+$ by preparing the ions in a pure magnetron or modified cyclotron state, letting them evolve freely during an accumulation time and then extracting them towards the detector
- Requires a position-sensitive detector ! (delay-line MCP)

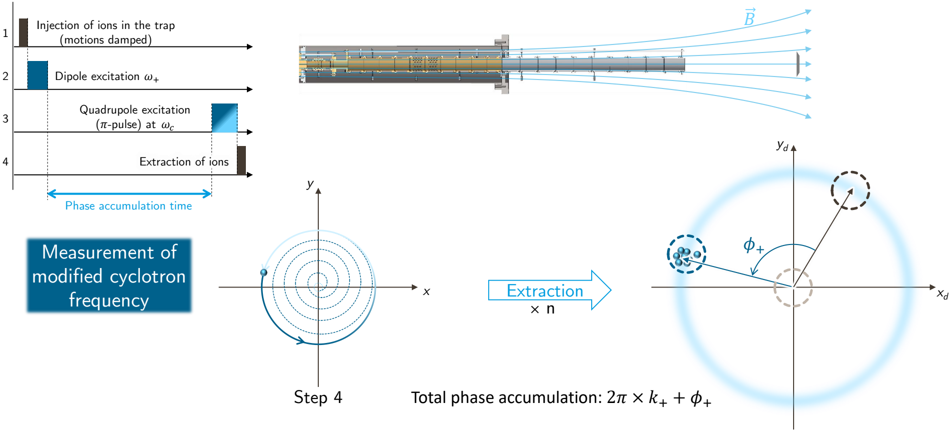

# Phase-imaging ion-cyclotron-resonance

- All ions are "useful"
- Higher resolving power
- Much easier to identify states that would be mixed in ToF methods

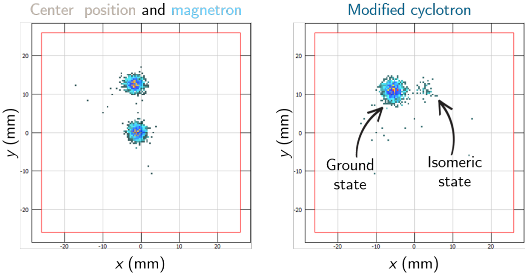


PI-ICR of $^{115}$Ru ions at JYFLTRAP (100ms accumulation time)

# Sideband cooling

Reminders :

- RIB are usually contaminated
- buffer gas axial and modified cyclotron motions are damped while magnetron motion is amplified

This can be exploited to remove contaminants in a "cocktail" bunch of ions !

# Sideband cooling

Reminders :

- RIB are usually contaminated
- buffer gas axial and modified cyclotron motions are damped while magnetron motion is amplified

This can be exploited to remove contaminants in a "cocktail" bunch of ions !

- Excitation of all ions with dipolar pulse at $\omega_-$ to a large $\rho_-$ orbit
- Quadrupole excitation at $\omega_c$ (mass-selective) is then applied to recenter only the ion of interest
- Ejection towards diaphragm $\Rightarrow$ only centered ions can go through
- Mass resolving power : $R \sim 10^5$

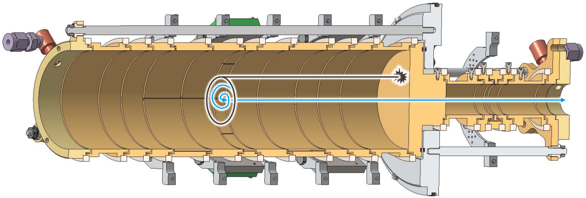

# Dipole cleaning at $\omega_+$

- Simply drive the contaminants far from the axis by exciting their modified cyclotron motion
- A dipole excitation at the contaminant's $\omega_+$ frequency is applied
- Can be done until the contaminant reaches the electrode radius but easier with a diaphragm
- Can be either broadband (short pulse and high amplitude) or high-resolution (long pulse and low amplitude)
- No gas needed but necessary to know what the contaminants are !
- $R$ up to $10^6$ possible depending on time available for excitation

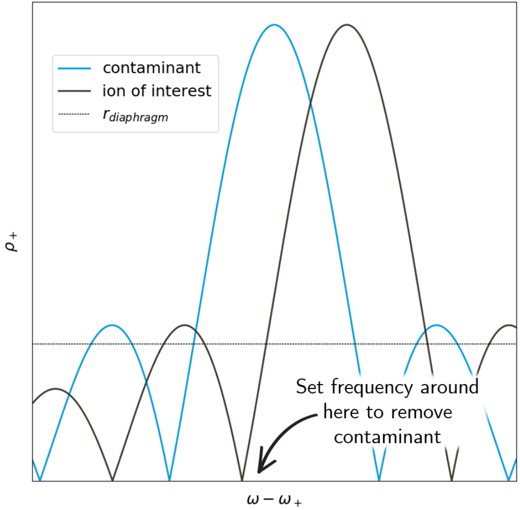

# Ramsey cleaning

- Same principle as the dipole cleaning but applying two (or more) pulses interleaved with waiting period(s)
- Higher resolving power (narrower linewidth)
- $R \sim$ a few $10^6$ possible depending on time available for excitation

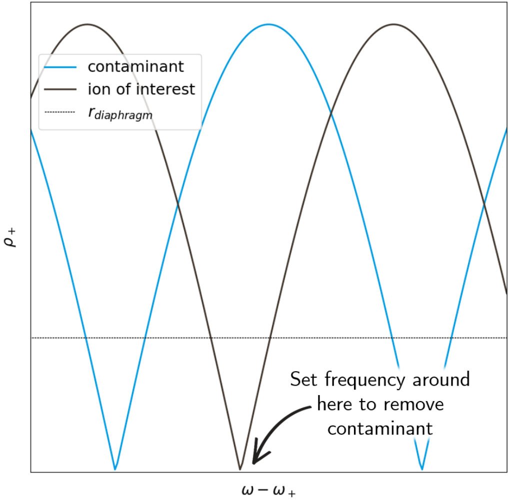

# PI-ICR cleaning

- Idea quite similar to the mass measurement technique
- Excite modified cyclotron motion
- Let contaminants accumulates phase difference with ion of interest
- Apply a dipole excitation at the right time to align ion of interest (only) with a collimator
- $R \sim$ a few $10^7$ reachable

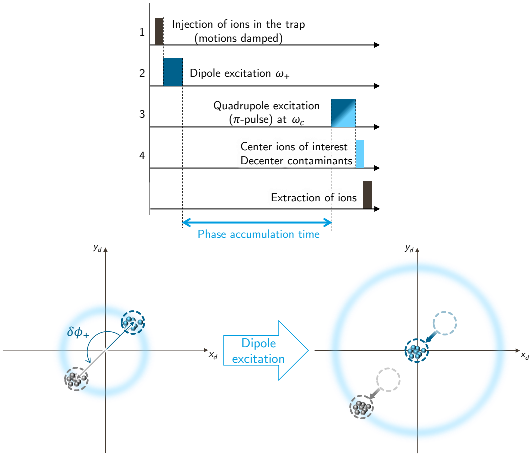

# MR-ToF MS

# Basic of ToF spectrometry

- Ions with different masses $m_i$ but same kinetic energy $K$ have different velocities
- Starting from a position at a given time, the heavier ions will hence take more time to travel through a given distance $d$

$$t_i = d\sqrt{\frac{m_i}{2K}} \Rightarrow R = \frac{m}{\Delta m} = \frac{t}{2\Delta t}$$

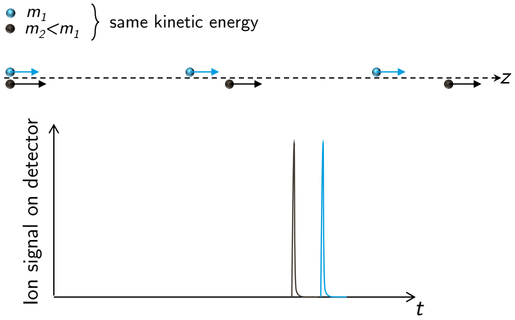


Resolution limited by path length $d$, energy dispersion $\Delta K$ and initial time dispersion $\Delta t_0$

# Reflectron

- Basic way to improve the ToF mass spectrometry : correct for energy dispersion
- By using an electrostatic mirror with growing voltages on a set of electrodes, the ions with a higher kinetic energy travels a longer way before getting reflected

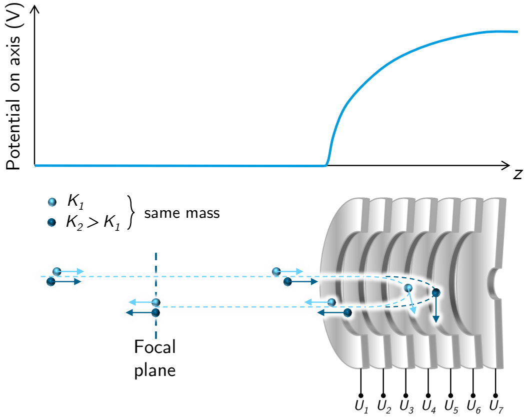

# MR-ToF MS

- First attempt to build a mass separator by the multi-reflection technique dates back to 1960 (residual gas analyzer)
- Very poor resolution !
- Ions produced directly inside the cavity

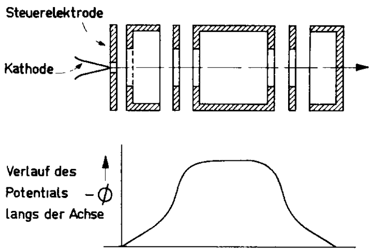


FIG 2. The arrangement of the electrodes and the shape of the electric potential $\phi$ along the axis

W. Tretner, Vacuum 10, 31 (1960)

$$R = \frac{M}{\Delta M} \approx 20$$

# MR-ToF MS

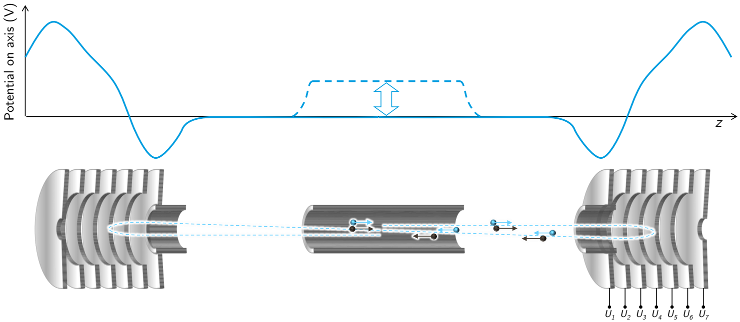


Ions enter the device ...

- either by switching potentials of the entrance mirror to values $U_i$ such that $qU_i < K$
- or by using a pulsed drift tube to lower the ions energy once inside

- Voltages tailored to achieve minimum bunch length on the detector or selection device
- Lens electrodes on each side for stable trajectories
- Mass resolving power $R \sim 10^5$

# MR-ToF MS

- $t = a\sqrt{\frac{m}{q}} + b$
- $a$ and $b$ must be determined by calibration with known masses $m_1$ and $m_2$

For an unknown ion mass $m$ having a ToF $t$ and known masses $m_i$ with ToF $t_i$ :

$$m = \left[ C_{ToF} \left( \sqrt{m_1} - \sqrt{m_2} \right) + \frac{1}{2} \left( \sqrt{m_1} + \sqrt{m_2} \right) \right]^2$$

where $C_{ToF} = \dfrac{2t - t_1 - t_2}{2(t_1 - t_2)}$

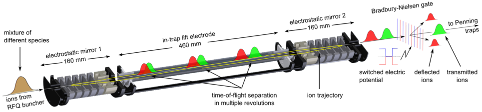


R. N. Wolf et al. NIM A 686, 82 (2012)

$$R = \frac{M}{\Delta M} \approx 2 \times 10^5$$

# Removing the contaminants

- The multi-reflections process separates spatially the species but does not provide the purification itself
- A Bradbury-Nielsen gate is used to remove the contaminants from the beam
- It relies on a fast switching of the voltage on a grid of thin wires

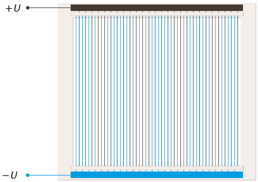

# Removing the contaminants

- The multi-reflections process separates spatially the species but does not provide the purification itself
- A Bradbury-Nielsen gate is used to remove the contaminants from the beam
- It relies on a fast switching of the voltage on a grid of thin wires
- Gate is open only for a small duration when ions of interest arrive on the BN gate

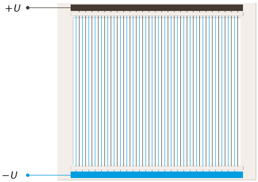


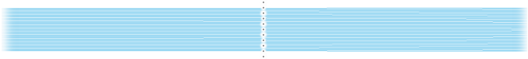

Gate opened

# Removing the contaminants

- The multi-reflections process separates spatially the species but does not provide the purification itself
- A Bradbury-Nielsen gate is used to remove the contaminants from the beam
- It relies on a fast switching of the voltage on a grid of thin wires
- Gate is open only for a small duration when ions of interest arrive on the BN gate
- The opposite voltages between neighbouring wires when gate is closed deflect the contaminants away from the beam axis
- Time focusing on the BN gate to get best $R$

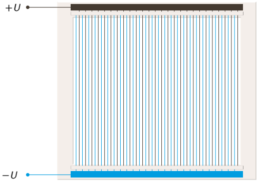


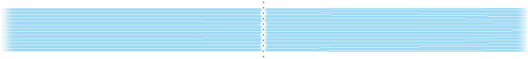

Gate opened

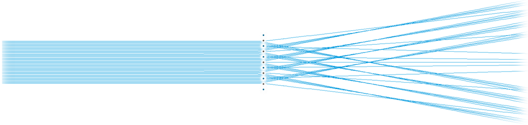

Gate closed

# What nuclear physics can be studied with traps ?

# Laser spectroscopy

Measurements of size, shape and electromagnetic moments of radioactive nuclei through hyperfine structure...

- Requires trap(s) to cool and bunch the ion bunches
- Benefits from the help of traps for identification (trap assisted laser spectroscopy)

## See Iain and Ruben's lectures

# Precision studies of the weak interaction through $\beta$ decays

Universality of the weak interaction ($W$ and $Z$ bosons interacts universally with all fermions, i.e. same coupling constant)

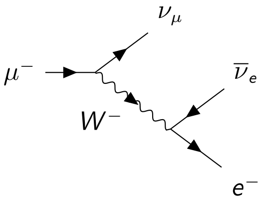


Purely leptonic decay

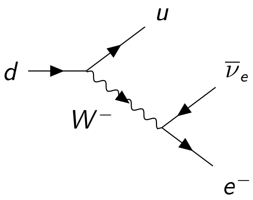


Semi-leptonic decay

Experimental values are pretty much the same...

# Precision studies of the weak interaction through $\beta$ decays

Universality of the weak interaction ($W$ and $Z$ bosons interacts universally with all fermions, i.e. same coupling constant)

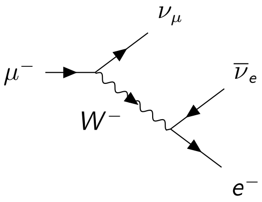


Purely leptonic decay

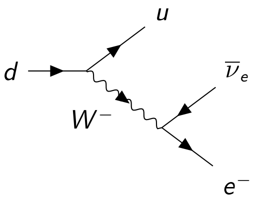


Semi-leptonic decay

Experimental values are pretty much the same...

... but not exactly

$$G_F = 1{,}166\,378\,7(6) \times 10^{-5}\,(\hbar c)^3/\mathrm{GeV}^2$$

$$G_V = 1{,}136(3) \times 10^{-5}\,(\hbar c)^3/\mathrm{GeV}^2 = 97{,}4\%\,G_F$$

# The CKM matrix

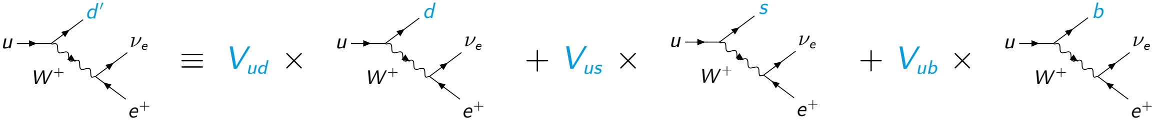


Without quark mixing, the 3 family would not be coupled $\underbrace{\begin{pmatrix} d' \\ s' \\ b' \end{pmatrix}}_{\text{Weak eigenstates}} = M_{CKM} \times \underbrace{\begin{pmatrix} d \\ s \\ b \end{pmatrix}}_{\text{Mass eigenstates}}$

# The CKM matrix

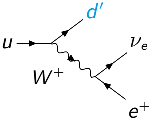


$\equiv V_{ud} \times$

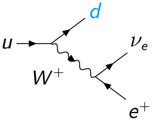


$+ V_{us} \times$

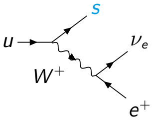


$+ V_{ub} \times$

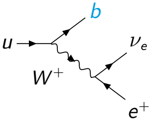


Without quark mixing, the 3 family would not be coupled $\underbrace{\begin{pmatrix} d' \\ s' \\ b' \end{pmatrix}}_{\text{Weak eigenstates}} = M_{CKM} \times \underbrace{\begin{pmatrix} d \\ s \\ b \end{pmatrix}}_{\text{Mass eigenstates}}$

$$M_{CKM} = \begin{pmatrix} V_{ud} & V_{us} & V_{ub} \\ V_{cd} & V_{cs} & V_{cb} \\ V_{td} & V_{ts} & V_{tb} \end{pmatrix} = \begin{pmatrix} 0.97373(31) & 0.22506(50) & 0.00357(15) \\ 0.22492(50) & 0.97351(13) & 0.0411(13) \\ 0.00875(^{+32}_{-33}) & 0.0403(13) & 0.99915(5) \end{pmatrix}$$

Values not predicted by the SM $\Rightarrow$ must be measured !

In the Standard Model, the Cabibbo-Kobayashi-Maskawa matrix has to be unitary

$$\Rightarrow V_{ud}^2 + V_{us}^2 + V_{ub}^2 = 1$$

# Compared half-lives

- $V_{ud}$ is by far the dominant term of the first row and column
- It is best measured using super-allowed $\beta^+$ transitions between $J^\pi = 0^+$ isobaric analog states
- To trace back to $V_{ud}$, 3 quantities are needed :
  - The energy $Q$ released in the decay
  - the half-life $T$ of the parent state
  - the branching ratio of the $\beta$ decay to the IAS

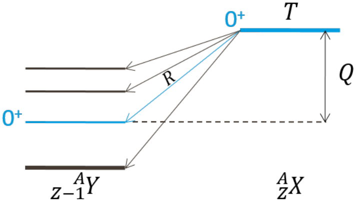


$$ft = f(Q)\frac{T}{R}\left(1+\frac{\varepsilon}{\beta}\right) = \frac{2\pi^3\hbar^7 \ln 2}{m_e c^4}\frac{1}{2G_F^2 {V_{ud}}^2}$$

# Compared half-lives

- $V_{ud}$ is by far the dominant term of the first row and column
- It is best measured using super-allowed $\beta^+$ transitions between $J^\pi = 0^+$ isobaric analog states
- To trace back to $V_{ud}$, 3 quantities are needed :
  - The energy $Q$ released in the decay
  - the half-life $T$ of the parent state
  - the branching ratio of the $\beta$ decay to the IAS

$$ft = f(Q)\frac{T}{R}\left(1+\frac{\varepsilon}{\beta}\right) = \frac{2\pi^3\hbar^7 \ln 2}{m_e c^4}\frac{1}{2G_F^2 {V_{ud}}^2}$$

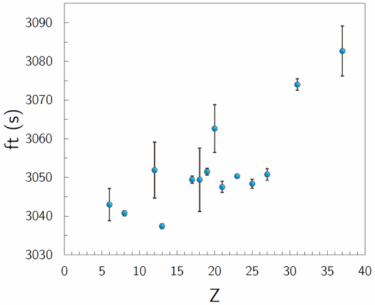


$ft$ constant at the % level

# Compared half-lives

- $V_{ud}$ is by far the dominant term of the first row and column
- It is best measured using super-allowed $\beta^+$ transitions between $J^\pi = 0^+$ isobaric analog states
- To trace back to $V_{ud}$, 3 quantities are needed :
  - The energy $Q$ released in the decay
  - the half-life $T$ of the parent state
  - the branching ratio of the $\beta$ decay to the IAS

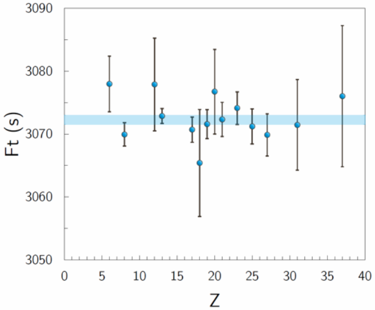


$$ft = f(Q)\frac{T}{R}\left(1+\frac{\varepsilon}{\beta}\right) = \frac{2\pi^3\hbar^7 \ln 2}{m_e c^4}\frac{1}{2G_F^2 {V_{ud}}^2}$$

$$\overline{Ft} = 3072{,}24(57)\,\mathrm{s} \Rightarrow \frac{\Delta\overline{Ft}}{\overline{Ft}} = 0.02\%$$

- However some theoretical corrections must be done to get a "true" constant :

$$Ft = ft\left(1+\delta'_R\right)\left(1+\delta_{NS}-\delta_C\right) = \frac{2\pi^3\hbar^7 \ln 2}{m_e c^4\left(1+\Delta_R\right)}\frac{1}{2G_F^2 {V_{ud}}^2}$$

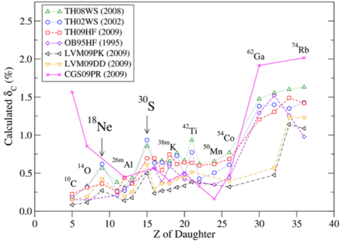

# Why are traps needed in this business

- All of the recent $Q$ values involved in the $0^+ \rightarrow 0^+$ study are directly measured with a Penning trap

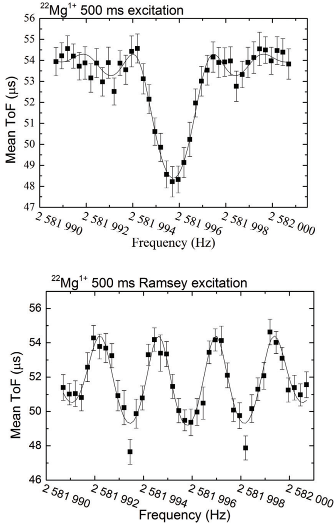


M. P. Reiter *et al.*, Phys. Rev. C 96, 052501(R) (2017)

# Why are traps needed in this business

- All of the recent $Q$ values involved in the $0^+ \to 0^+$ study are directly measured with a Penning trap
- When measuring the half-life or branching ratio, purity of the collected sample of nuclei is crucial to get results precise at the ‰ level
- This is especially true when the beta feeding is highly fragmented leading to many weak branches (Pandemonium effect)

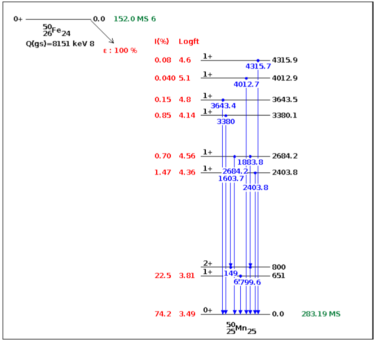


extracted from the NuDat 2 database

# Nuclear structure studies

- Mass measurement gives direct access to particle separation energies

$$S_{2n} = [\mathcal{M}(A-2,Z) + 2\mathcal{M}(n) - \mathcal{M}(A,Z)]\, c^2$$

- Trends in the evolution of these particle separation energies are good indicators of structure effects
- Sudden changes in the trends reveal shell closures or nuclear shape change

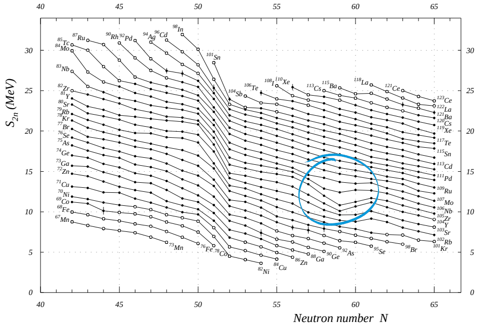


Adapted from M. Wang *et al.*, Chinese Physics C 45, 3, 030003 (2021)

# Nuclear structure studies

- Close to $^{100}$Sn, heaviest $N = Z$ nucleus
- $\mathcal{M}(^{100}\mathrm{Sn})$ deduced from $\mathcal{M}(^{100}\mathrm{In})$ and $Q_\beta$ measurements at GSI and RIKEN (at odds)
- $^{99-101}$In produced at ISOLDE and studied with ISOLTRAP
  - Cooling and bunching with the RFQ
  - Purification with the MR-ToF MS
  - Mass measurement
    - with the MR-ToF MS $^{99}$In (low yield)
    - with Ramsey-ToF ($^{100}$In)
    - with PI-ICR ($^{101}$In)
- Questions validity of either the expected trends for a doubly magic nucleus or the most precise measurement of $^{100}$Sn

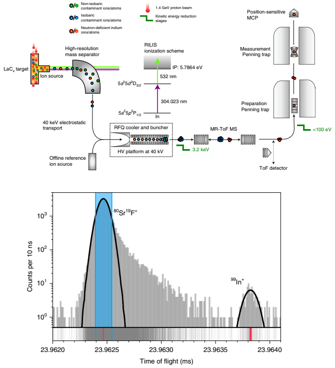


M. Mougeot *et al.*, Nat. Phys.(2021)

https://doi.org/10.1038/s41567-021-01326-9

# Nuclear structure studies

- Close to $^{100}$Sn, heaviest $N = Z$ nucleus
- $\mathcal{M}(^{100}\mathrm{Sn})$ deduced from $\mathcal{M}(^{100}\mathrm{In})$ and $Q_\beta$ measurements at GSI and RIKEN (at odds)
- $^{99-101}$In produced at ISOLDE and studied with ISOLTRAP
  - Cooling and bunching with the RFQ
  - Purification with the MR-ToF MS
  - Mass measurement
    - with the MR-ToF MS $^{99}$In (low yield)
    - with Ramsey-ToF ($^{100}$In)
    - with PI-ICR ($^{101}$In)
- Questions validity of either the expected trends for a doubly magic nucleus or the most precise measurement of $^{100}$Sn

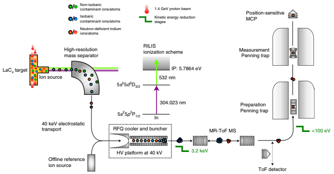


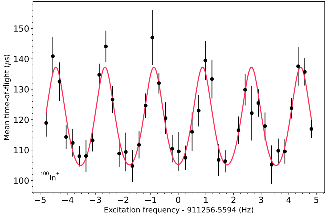


M. Mougeot *et al.*, Nat. Phys.(2021)

https://doi.org/10.1038/s41567-021-01326-9

# Nuclear structure studies

- Close to $^{100}$Sn, heaviest $N = Z$ nucleus
- $\mathcal{M}(^{100}\mathrm{Sn})$ deduced from $\mathcal{M}(^{100}\mathrm{In})$ and $Q_\beta$ measurements at GSI and RIKEN (at odds)
- $^{99-101}$In produced at ISOLDE and studied with ISOLTRAP
  - Cooling and bunching with the RFQ
  - Purification with the MR-ToF MS
  - Mass measurement
    - with the MR-ToF MS $^{99}$In (low yield)
    - with Ramsey-ToF ($^{100}$In)
    - with PI-ICR ($^{101}$In)
- Questions validity of either the expected trends for a doubly magic nucleus or the most precise measurement of $^{100}$Sn

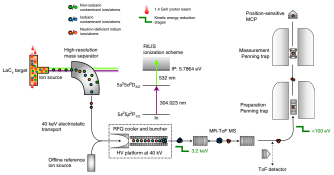


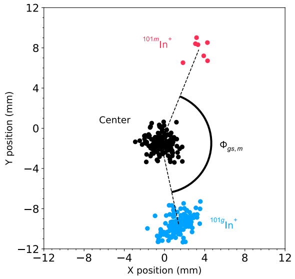


M. Mougeot *et al.*, Nat. Phys.(2021)

https://doi.org/10.1038/s41567-021-01326-9

# Nuclear structure studies

- Close to $^{100}$Sn, heaviest $N = Z$ nucleus
- $\mathcal{M}(^{100}\mathrm{Sn})$ deduced from $\mathcal{M}(^{100}\mathrm{In})$ and $Q_\beta$ measurements at GSI and RIKEN (at odds)
- $^{99-101}$In produced at ISOLDE and studied with ISOLTRAP
    - Cooling and bunching with the RFQ
    - Purification with the MR-ToF MS
    - Mass measurement
        - with the MR-ToF MS $^{99}$In (low yield)
        - with Ramsey-ToF ($^{100}$In)
        - with PI-ICR ($^{101}$In)
- Questions validity of either the expected trends for a doubly magic nucleus or the most precise measurement of $^{100}$Sn

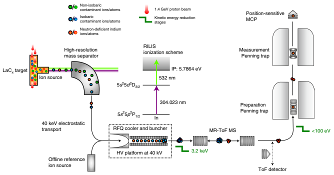


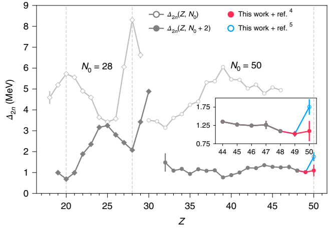


M. Mougeot *et al.*, Nat. Phys.(2021)

https://doi.org/10.1038/s41567-021-01326-9

# Mass measurements for nuclear astrophysics

- Roughly half of the natural abundance of the heavy elements produced by processes taking place far from stability

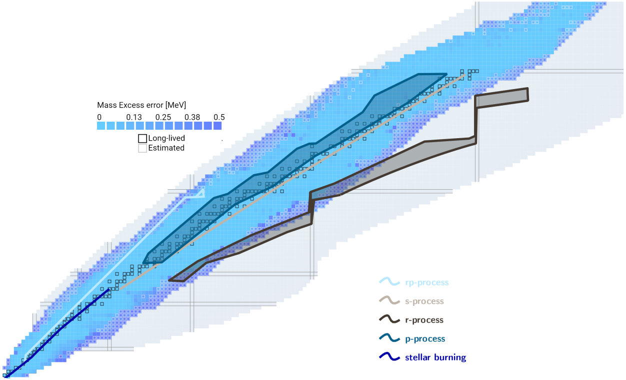

# Mass measurements for nuclear astrophysics

- Roughly half of the natural abundance of the heavy elements produced by processes taking place far from stability
- Most of it due to r-process but astrophysical sites where it happens still debated

LETTER

doi:10.1038/nature24453

## Origin of the heavy elements in binary neutron-star mergers from a gravitational-wave event

Daniel Kasen[1,2], Brian Metzger[3], Jennifer Barnes[3], Eliot Quataert[1] & Enrico Ramirez-Ruiz[4,5]

**The cosmic origin of elements heavier than iron has long been uncertain. Theoretical modelling[1–7] shows that the matter that is expelled in the violent merger of two neutron stars can assemble into heavy elements such as gold and platinum in a process known as rapid neutron capture (r-process) nucleosynthesis. The radioactive decay of isotopes of the heavy elements is predicted[8–12] to power a distinctive thermal glow (a 'kilonova'). The discovery of an electromagnetic counterpart to the gravitational-wave source[13] GW170817 represents the first opportunity to detect and scrutinize a sample of freshly synthesized r-process elements[14–18]. Here we report models that predict the electromagnetic emission of kilonovae in detail and enable the mass, velocity and composition of ejecta to be derived from observations. We compare the models to the optical and infrared radiation associated with the GW170817 event to argue that the observed source is a kilonova. We infer the presence of two distinct components of ejecta, one composed primarily of light (atomic mass number less than 140) and one of heavy (atomic mass number greater than 140) r-process elements. The ejected mass and a merger rate inferred from GW170817 imply that such mergers are a dominant mode of r-process production in the Universe.**

The discovery[13] by the LIGO–Virgo experiments of gravitational waves from inspiralling neutron stars triggered an extensive campaign of follow-up observations, and the detection of counterpart emission across the electromagnetic spectrum. At optical and infrared wavelengths, the counterpart to GW170817 (originally announced by the Swope team[18] and called 'SSS17a', and hereafter referred to by its IAU designation AT 2017gfo) has properties that differ from previously known astrophysical transients. A day after the merger, the source was optically bright (with luminosity of about $10^8$ times that of the Sun at wavelengths of about 0.5 μm), but it faded rapidly within days[14–16]. Meanwhile, the emission in the infrared (1–3 μm) remained bright for nearly two weeks[15–19]. The spectra of AT 2017gfo were quasi-blackbody, suggestive of a thermal source[20,21].

The characteristics of AT 2017gfo—its rapid optical evolution[8], long-lived infrared emission[11,12] and luminosity consistent with radioactive r-process heating[9,10]—resemble theoretical predictions for kilonovae. To explore this identification, we present here a survey of models of the radioactive aftermath of a neutron-star merger. The key parameters of the models are the ejected mass $M$, characteristic expansion velocity $v_k$, and the composition of ejected matter. The ejecta is freely expanding (radius equal to the product of velocity and time, $R = vt$) and the density profile is described by a broken power law (see Methods). We synthesize model observables by numerically solving the Boltzmann equation for relativistic radiation transport in a radioactive plasma. We self-consistently calculate the thermal and ionization/excitation state of the ejecta and derive the wavelength-dependent opacity and emissivity using atomic-structure model data for multiple ions (see Methods). The validity of the transport method has been established by previous modelling of supernovae of all types.

We explore models motivated by general-relativistic simulations of mergers, which identify two distinct mechanisms for mass ejection (see Fig. 1). First, matter may be dynamically expelled on a timescale of milliseconds during the merger itself. Tidal forces peel matter from

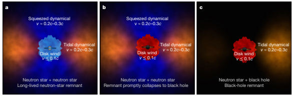


**Figure 1 | Schematic illustration of the components of matter ejected from neutron-star mergers.** Red colours denote regions of heavy r-process elements, which radiate red/infrared light. Blue colours denote regions of light r-process elements which radiate blue/optical light. During the merger, tidal forces peel off tails of matter, forming a torus of heavy r-process ejecta in the plane of the binary. Material squeezed into the polar regions during the stellar collision can form a cone of light r-process material. Roughly spherical winds from a remnant accretion disk can also contribute, and are sensitive to the fate of the central merger remnant. **a**, If the remnant survives as a hot neutron star for tens of milliseconds, its neutrino irradiation lowers the neutron fraction and produces a blue wind. **b**, If the remnant collapses promptly to a black hole, neutrino irradiation is suppressed and the winds may be red. **c**, In the merger of a neutron star and a black hole, only a single tidal tail is ejected and the disk winds are more likely to be red.

[1]Departments of Physics and Astronomy, and Theoretical Astrophysics Center, University of California, Berkeley, California 94720-7300, USA. [2]Nuclear Science Division, Lawrence Berkeley National Laboratory, Berkeley, California 94720-8169, USA. [3]Department of Physics and Columbia Astrophysics Laboratory, Columbia University, New York, New York 10027, USA. [4]Department of Astronomy, University of Santa Cruz, California, USA. [5]DARK, Niels Bohr Institute, University of Copenhagen, Blegdamsvej 17, 2100 Copenhagen, Denmark.

80 | NATURE | VOL 551 | 2 NOVEMBER 2017

# Mass measurements for nuclear astrophysics

- Roughly half of the natural abundance of the heavy elements produced by processes taking place far from stability
- Most of it due to r-process but astrophysical sites where it happens still debated
- Final abundances depends on site characteristics : temperature, density, neutron richness,etc. and the balance between rates of
  - $(n, \gamma)$
  - $(\gamma, n)$
  - $\beta$ decay
  - $\beta$-delayed $n$ emission
  - (fission)

  all along the path

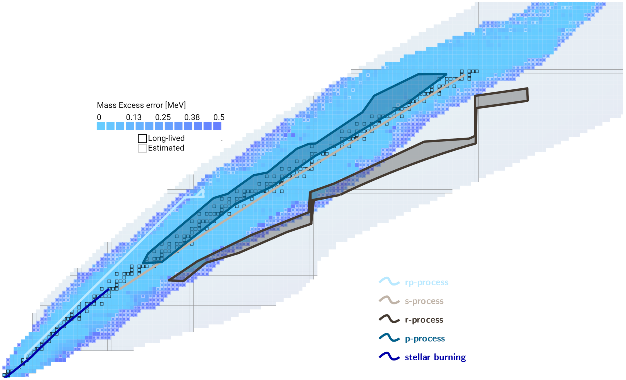

# Mass measurements for nuclear astrophysics

- Each of the potential r-process site have distinct characteristics
- One could expect the final abundance pattern should then point out the production site

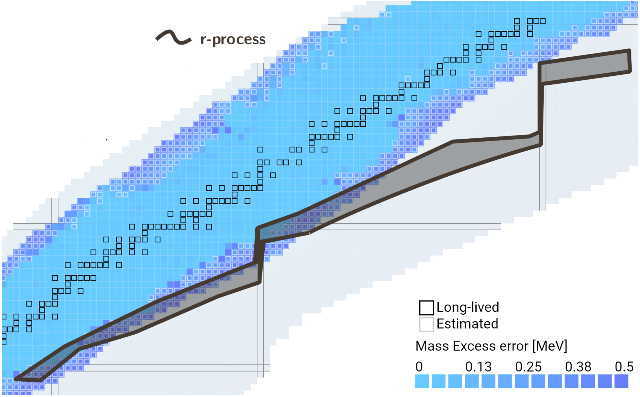

# Mass measurements for nuclear astrophysics

- Each of the potential r-process site have distinct characteristics
- One could expect the final abundance pattern should then point out the production site
- Most of the process takes place in very poorly or even not known regions of the nuclide chart
- Uncertainties make the calculations accuracy too low for precise predictions

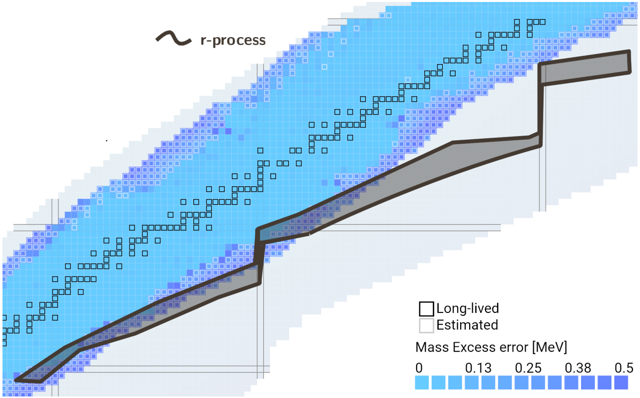

# Mass measurements for nuclear astrophysics

- Each of the potential r-process site have distinct characteristics
- One could expect the final abundance pattern should then point out the production site
- Most of the process takes place in very poorly or even not known regions of the nuclide chart
- Uncertainties make the calculations accuracy too low for precise predictions
- It is then crucial to decrease the uncertainties, especially on mass values (and the mass models based on knwon masses)

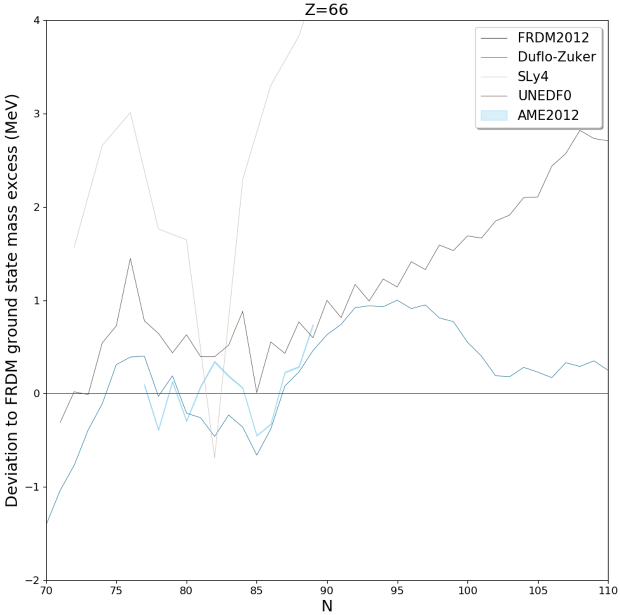

# Mass measurements for nuclear astrophysics

- Sensitivity studies highlight the impact of nuclei around $^{132}$Sn
- Several experiments done to improve precision of the masses in this region (often known only through $\beta$-decay endpoint before)

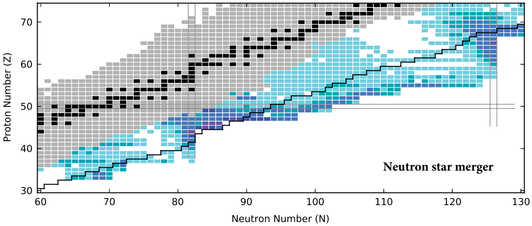


M.R. Mumpower *et al.*, Prog. Part. Nucl. Phys. 86, 86126 (2016)

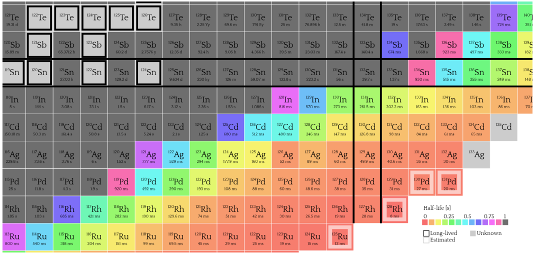

# Mass measurements for nuclear astrophysics

- Sensitivity studies highlight the impact of nuclei around $^{132}$Sn
- Several experiments done to improve precision of the masses in this region (often known only through $\beta$-decay endpoint before)

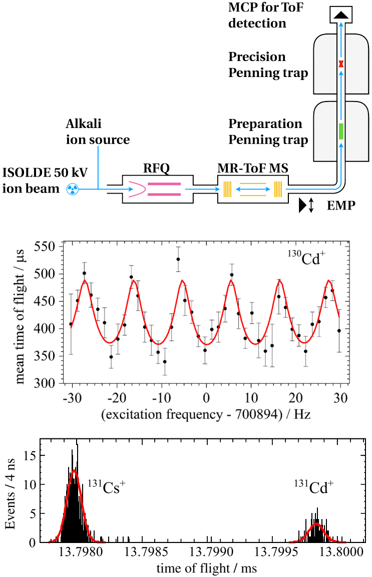


D. Atanasov *et al.*, Phys. Rev. Lett. 115, 232501 (2015)

# Mass measurements for nuclear astrophysics

- Sensitivity studies highlight the impact of nuclei around $^{132}$Sn
- Several experiments done to improve precision of the masses in this region (often known only through $\beta$-decay endpoint before)

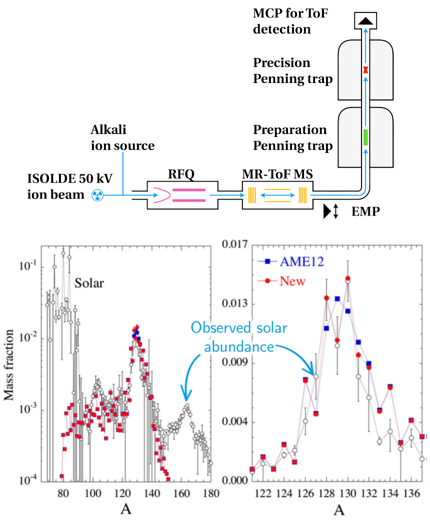


D. Atanasov *et al.*, Phys. Rev. Lett. 115, 232501 (2015)

# Mass measurements for nuclear astrophysics

- Sensitivity studies highlight the impact of nuclei around $^{132}$Sn
- Several experiments done to improve precision of the masses in this region (often known only through $\beta$-decay endpoint before)

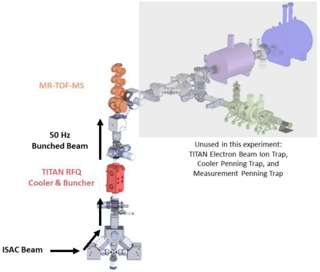


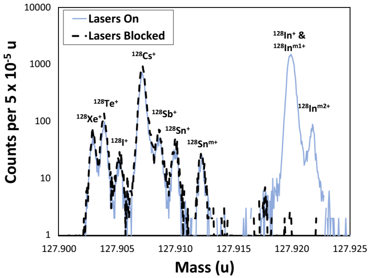


M. P. Reiter *et al.*, Phys. Rev. C 101, 025803 (2020)

# Mass measurements for nuclear astrophysics

- Sensitivity studies highlight the impact of nuclei around $^{132}$Sn
- Several experiments done to improve precision of the masses in this region (often known only through $\beta$-decay endpoint before)
- New network calculation needed to see the impact on r-process abundances but many new values with some 10 keV since AME2016 !

# Conclusion

- Hope you are convinced that traps are powerful tools for nuclear physics studies
- More than 30 years of trapping for nuclear physics but still very dynamic field

# Conclusion

- Hope you are convinced that traps are powerful tools for nuclear physics studies
- More than 30 years of trapping for nuclear physics but still very dynamic field
- Several new traps and new RIB-facilities are about to start up in coming years

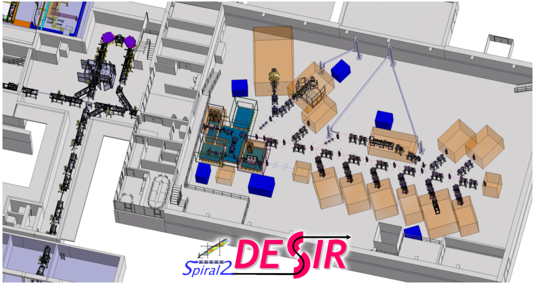


Exciting time to come !